

Analytic Sequential Weiss–Weinstein Bounds

Florian Xavier, Peter Gerstoft, Gerald Matz, *Senior Member, IEEE*, and
Christoph F. Mecklenbräuker, *Senior Member, IEEE*

Abstract—In this paper, we explore a sequential Bayesian bound for state-space models focusing on hybrid continuous and discrete random states. We provide an analytic recursion for the sequential Weiss–Weinstein (SWW) bound for linear state-space models with solutions for Gaussian, uniform, and exponential distributions as derived, as well as for a combination of these. We compare the SWW bound for discretized states with the corresponding bound for the continuous states. The SWW bound is contrasted with the sequential Cramér–Rao bound for Gaussian distributions. Practical issues of SWW bounds are discussed and numerical simulation results provide insights into their behavior.

Index Terms—Analytic sequential Weiss–Weinstein lower bound, Bayesian estimation, exponential distributions, uniform distributions, Gaussian distributions.

I. INTRODUCTION

RECENT investigations in the area of joint field and state estimation can be categorized as deterministic [1]–[3] and stochastic [4]–[8] approaches. In this paper, we follow a stochastic approach in a Bayesian framework. The study of lower bounds on the mean-square error matrix of a Bayesian estimator [9]–[12] entails various bounds [13]–[16].

We are interested in a Bayesian lower bound for state estimators which are applicable jointly to discrete and continuous random state variables. Additionally, the bound shall support the corresponding probability densities with finite support. Discretization of physical models described by partial differential equations [4], [5] or by static formulations induce discretized states [17]. These models often feature loosely coupled state variables. Due to the loose coupling, these models are interpreted as reduced-order models. Sequential Cramér–Rao (SCR) bounds were developed [6], [18] for continuous random states. It turns out that the regularity conditions for the applicability of the Bayesian Cramér–Rao (CR) bound are too restrictive for discrete states [19]. We seek bounds with relaxed regularity conditions which are applicable to discrete state variables. This requirement guides us to the Weiss–Weinstein (WW) bound [13],

Manuscript received January 29, 2013; revised June 04, 2013; accepted July 04, 2013. Date of publication July 18, 2013; date of current version September 11, 2013. The associate editor coordinating the review of this manuscript and approving it for publication was Dr. Petr Tichavsky. This work is funded by “Wiener Wissenschafts-, Forschungs- und Technologiefonds” (WWTF), Grant ICT08-44.

F. Xavier, G. Matz, and C. F. Mecklenbräuker are with the Institute of Telecommunications (ICT), Faculty of Electrical Engineering and Information Technology, Vienna University of Technology, 1040 Vienna, Austria (e-mail: fxaver@nt.tuwien.ac.at; gmatz@nt.tuwien.ac.at; cfm@nt.tuwien.ac.at)

P. Gerstoft is with the Scripps Institution of Oceanography, University of California, San Diego, La Jolla, CA 92093 USA (e-mail: gerstoft@ucsd.edu).

Color versions of one or more of the figures in this paper are available online at <http://ieeexplore.ieee.org>.

Digital Object Identifier 10.1109/TSP.2013.2273886

[15], [20], [21]. The temporal evolution of states is described by a state-space model and motivates the extension of the WW bound to a sequential formulation (SWW) [22], [23].

Apart from the underlying theory of SWW bounds [23], [24] and the application to fault-prone systems [25], [26], we are not aware of any explicit analytic results for specific probability densities nor their rigorous derivations.

This paper is organized as follows. In Section II, the use of the WW bound is introduced leading to the general formulation of the SWW bound. In addition to the referenced literature, we motivate the use of the SWW bound for hybrid continuous/discrete distributions and densities with finite support. We provide a general description of the bound utilizing the expectation operator. Furthermore, we emphasize foundations, which we need for the proofs in the subsequent sections. After definitions of discretized and hybrid models in Section III, key contributions of our paper follow:

- We provide an analytic SWW recursion for a linear state-space model (Section IV).
- The SWW bound for Gaussian distributions (Section IV), uniform distributions (Section V), and exponential distributions (Section VI) is presented.
- The SWW bound for discrete models, where the discrete states stem from discretization of continuous states (Section III to Section VI).
- Practical issues are addressed in Section VII: special prior distributions, the choice of SWW’s test point matrices, the computational effort, and partly deterministic noise.
- The final example (Section VIII) demonstrates the SWW bound for a three-dimensional state-space model for different probability distributions and compares them to a Bayesian filter (Kalman or particle filter).

Several lemmas are summarized and proved in the Appendices.

II. BAYESIAN LOWER BOUNDS

This section is inspired by [13], [23]–[26] and introduces the sequential SWW bound. We address hybrid discrete/continuous state vectors and emphasize properties for subsequent sections.

A. Preliminaries on Probability Theory

Let us assume a probability space $(\mathbb{R}^N, \mathcal{B}, P_{\mathbf{x}})$ with the sample space \mathbb{R}^N , the Borel algebra \mathcal{B} and the measure $P_{\mathbf{x}} : \mathcal{B} \rightarrow [0, 1]$. The expectation of a function $g(\mathbf{x})$ is defined using the probability measure $P_{\mathbf{x}}(\mathcal{B}) = P\{\mathbf{x} \in \mathcal{B}\}$ by

$$E_{\mathbf{x}}\{g(\mathbf{x})\} \triangleq \int_{\mathbb{R}^N} g(\mathbf{x}) dP_{\mathbf{x}}(\mathbf{x}). \quad (1)$$

We assume a probability measure consisting of a continuous $P_{\mathbf{x}}^c$ and a discrete $P_{\mathbf{x}}^d$ part [27], [28], i.e.,

$$P_{\mathbf{x}} = c_1 P_{\mathbf{x}}^c + c_2 P_{\mathbf{x}}^d, \quad (2)$$

with $c_1 + c_2 = 1, c_1 \in [0, 1]$. Inserting (2) into (1), the latter one splits into one integral with Lebesgue measure $\lambda^c([a_1, b_1] \times \dots \times [a_N, b_N]) = (b_1 - a_1) \dots (b_N - a_N)$ and another one with counting measure $\lambda_{\mathcal{C}}^d(\mathcal{A}) = \sum_{\ell \in \mathcal{C}} \mathbb{1}_{\ell}(\mathcal{A})$ where $\mathcal{C} \in \mathcal{B}$ and $\mathbb{1}$ is the indicator function. We arrive at

$$\int_{\mathbb{R}^N} c_1 g(\mathbf{x}) f_{\mathbf{x}}(\mathbf{x}) d\mathbf{x} + \sum_{\mathbf{x} \in \mathcal{C}} c_2 g(\mathbf{x}) p_{\mathbf{x}}(\mathbf{x}) \quad (3)$$

with the probability density function (PDF) $f_{\mathbf{x}}(\mathbf{x}) = dP_{\mathbf{x}}^c(\mathbf{x})/d\lambda^c(\mathbf{x})$ and the probability mass function (PMF) $p_{\mathbf{x}}(\mathbf{x}) = dP_{\mathbf{x}}^d(\mathbf{x})/d\lambda_{\mathcal{C}}^d(\mathbf{x})$.

B. Bayesian Bounds

In the following, we denote a hybrid continuous/discrete probability density by $v_{\mathbf{x}}(\mathbf{x}) = c_1 f_{\mathbf{x}}(\mathbf{x}) + c_2 p_{\mathbf{x}}(\mathbf{x}), c_1 \in [0, 1], c_1 + c_2 = 1$ and call it simply probability density (PD). Especially when no measure is specified this notation allows the consideration of continuous and discrete random variables. We use the notation $d\lambda_{\mathbf{x}}$ whenever we assume the existence of a density for the random variable \mathbf{x} . To simplify notation, we use $\mathbb{E}\{\cdot\} \triangleq \mathbb{E}_{\mathbf{x}, \mathbf{y}}\{\cdot\}, f(\mathbf{x}) \triangleq f_{\mathbf{x}}(\mathbf{x}), p(\mathbf{x}) \triangleq p_{\mathbf{x}}(\mathbf{x})$ and $v(\mathbf{x}) \triangleq v_{\mathbf{x}}(\mathbf{x})$. In the sequel, \mathbf{x} is the N -dimensional parameter vector to be inferred from the perturbed measurements

$$\mathbf{y} = C(\mathbf{x}) + \mathbf{v}, \quad \mathbf{x} \sim v(\mathbf{x}), \quad \mathbf{v} \sim v(\mathbf{v}), \quad (4)$$

with a mapping C and measurement noise \mathbf{v} . The resulting estimation error of estimate $\hat{\mathbf{x}}$ is defined by

$$\boldsymbol{\varepsilon} \triangleq \hat{\mathbf{x}}(\mathbf{y}) - \mathbf{x}. \quad (5)$$

The Bayesian lower bound is a lower bound for the mean-square error (MSE) of any Bayesian estimator. With $\mathbf{g}(\mathbf{x}, \mathbf{y})$ being a real-valued measurable function satisfying $\mathbb{E}_{\mathbf{x}}\{\mathbf{g}(\mathbf{x}, \mathbf{y})\} = \mathbf{0}$, the mean-square error matrix [13] is lower bounded by

$$\mathbb{E}\{\boldsymbol{\varepsilon}\boldsymbol{\varepsilon}^T\} \succcurlyeq \mathbb{E}\{\mathbf{y}\mathbf{y}^T\} \mathbb{E}\{\mathbf{g}\mathbf{g}^T\}^{-1} \mathbb{E}\{\mathbf{y}\mathbf{g}^T\}^T \quad (6)$$

where $\mathbb{E}\{\mathbf{g}\mathbf{g}^T\}$ is a non-singular matrix. The elements of all matrix must be finite. The relational operator \succcurlyeq indicates that the difference between left and right hand sides is a positive semi-definite matrix. The function $\mathbf{g}(\mathbf{x}, \mathbf{y})$ is a *sensitivity function* termed *score* which defines specific Bayesian bounds.

1) *Cramér–Rao Bound and Bobrovsky–Zakai Bound*: For the Cramér–Rao lower bound (CR) the score of a continuous random parameter \mathbf{x} is defined by

$$\mathbf{g}(\mathbf{x}, \mathbf{y}) = \partial_{\mathbf{x}} \ln f(\mathbf{x}, \mathbf{y}) = \frac{\partial_{\mathbf{x}} v(\mathbf{x}, \mathbf{y})}{v(\mathbf{x}, \mathbf{y})} \quad (7)$$

with the assumption that $\lim_{|\mathbf{x}|_{\ell} \rightarrow \pm\infty} [\mathbf{x}]_{\ell} f(\mathbf{x}|\mathbf{y}) = 0$ for all $\ell = 1, \dots, N$ and \mathbf{y} . The ℓ th element of \mathbf{x} is denoted by $[\mathbf{x}]_{\ell}$. Furthermore, the first and second derivatives of $f(\mathbf{x}, \mathbf{y})$ with respect to \mathbf{x} must exist and be absolutely integrable. Inserting (7) into (6) gives [13]

$$\mathbb{E}\{\boldsymbol{\varepsilon}\boldsymbol{\varepsilon}^T\} \succcurlyeq \mathbb{E}\{\mathbf{g}(\mathbf{x}, \mathbf{y})\mathbf{g}(\mathbf{x}, \mathbf{y})^T\}^{-1} \triangleq \mathbf{J}^{-1} \quad (8)$$

with \mathbf{J} being the Bayesian information matrix.

For discrete \mathbf{x} , the $\partial_{\mathbf{x}}$ in (7) is approximated by the difference quotient

$$\frac{1}{\mathbf{h}} \Delta_{\mathbf{x}} v(\mathbf{x}) \triangleq \left(\frac{1}{h_1} \Delta_{x_1} v(\mathbf{x}), \dots, \frac{1}{h_N} \Delta_{x_N} v(\mathbf{x}) \right)^T \quad (9)$$

where $\frac{1}{h_{\ell}} \Delta_{x_{\ell}} v(\mathbf{x}) \triangleq (v(\mathbf{x} + h_{\ell} \mathbf{e}_{\ell}) - v(\mathbf{x})) / h_{\ell}$, and only the ℓ th elements of the unit vector \mathbf{e}_{ℓ} is unity. Variables h_{ℓ} specify the sample period if the densities are discrete approximations of continuous ones. This allows the use of hybrid continuous/discrete densities $v(\mathbf{x}, \mathbf{y})$. One alternative to the score (7) is

$$\partial_{\mathbf{x}} \ln v(\mathbf{x}, \mathbf{y}) \approx \frac{1}{v(\mathbf{x}, \mathbf{y})} \frac{1}{\mathbf{h}} \Delta_{\mathbf{x}} v(\mathbf{x}, \mathbf{y}) = \mathbf{g}(\mathbf{x}, \mathbf{y}) \quad (10)$$

with $\mathbf{h} = [h_1, \dots, h_N]^T \in \mathbb{R}^N$. This score is a special case of Bobrovsky and Zakai's [29] (BZ) choice of score,

$$g_u = L(\mathbf{x} + \mathbf{h}_u, \mathbf{x}, \mathbf{y}) - 1 \quad u = 1, \dots, N. \quad (11)$$

Here, L is the *likelihood ratio*

$$L(\mathbf{x}_1, \mathbf{x}_2, \mathbf{y}) \triangleq \frac{v(\mathbf{x}_1, \mathbf{y})}{v(\mathbf{x}_2, \mathbf{y})} = \frac{v(\mathbf{x}_1, \mathbf{y})}{\tilde{v}(\mathbf{x}_1, \mathbf{y})} = \frac{dP_{\mathbf{x}, \mathbf{y}}^{(1)}}{dP_{\mathbf{x}, \mathbf{y}}^{(2)}} \quad (12)$$

which is equivalent to the Radon–Nikodym derivative of probability measure $P^{(1)}$ with respect to $P^{(2)}$. The BZ lower bound is [29]

$$\mathbb{E}\{\boldsymbol{\varepsilon}\boldsymbol{\varepsilon}^T\} \succcurlyeq \mathbf{H}\mathbf{J}^{-1}\mathbf{H}^T \quad (13)$$

where

$$[\mathbf{J}]_{ab} := \mathbb{E}\{L(\mathbf{x} + \mathbf{h}_a, \mathbf{x}, \mathbf{y})L(\mathbf{x} + \mathbf{h}_b, \mathbf{x}, \mathbf{y})\} - 1, \quad (14)$$

$$\mathbf{H} \triangleq [\mathbf{h}_1, \dots, \mathbf{h}_N], \quad a, b = 1, \dots, N. \quad (15)$$

The specific choices of the *test points* \mathbf{h}_a and \mathbf{h}_b influence the lower bound on the mean-square error of elements a and b .

The Radon–Nikodym derivative (12) exists if and only if $P^{(1)}$ is absolutely continuous with respect to $P^{(2)}$. This means that the support of \tilde{v} is part of the support of v . This is not the case for truncated densities such as the uniform density. Thus a more general bound is necessary.

2) *Weiss–Weinstein Bound*: The Weiss–Weinstein (WW) lower bound is a generalization of the BZ bound. In the sequel, we use the score

$$g_u(\mathbf{x}, \mathbf{y}) = \sqrt{L(\mathbf{x} + \mathbf{h}_u, \mathbf{x}, \mathbf{y})} - \sqrt{L(\mathbf{x} - \mathbf{h}_u, \mathbf{x}, \mathbf{y})} \quad (16)$$

where $u = 1, \dots, N$ (cf. [13], [20], [30] with $s_1 = s_2 = 1/2$). Inserting (16) into (6), the WW bound is given by

$$\mathbb{E}\{\boldsymbol{\varepsilon}\boldsymbol{\varepsilon}^T\} \succcurlyeq \mathbf{H}\mathbf{J}^{-1}\mathbf{H}^T \quad (17)$$

where

$$[\mathbf{J}]_{ab} := 2 \frac{e^{\mu(\mathbf{h}_a, -\mathbf{h}_b)} - e^{\mu(\mathbf{h}_a, \mathbf{h}_b)}}{e^{\mu(\mathbf{h}_a, \mathbf{0})} e^{\mu(\mathbf{0}, \mathbf{h}_b)}}, \quad (18)$$

with the negative non-metric Bayesian *Bhattacharyya distance* (BD) between $v(\mathbf{x} + \mathbf{h}_a, \mathbf{y})$ and $v(\mathbf{x} - \mathbf{h}_b, \mathbf{y})$, [31], [32],

$$\mu(\mathbf{h}_a, \mathbf{h}_b) = \ln \mathbb{E} \left\{ \frac{\sqrt{v(\mathbf{x} + \mathbf{h}_a, \mathbf{y})v(\mathbf{x} - \mathbf{h}_b, \mathbf{y})}}{v(\mathbf{x}, \mathbf{y})} \right\}. \quad (19)$$

The corresponding Bayesian Bhattacharyya coefficient

$$\rho = \exp(\mu(\mathbf{h}_a, \mathbf{h}_b)) \quad (20)$$

lies between zero and unity. The more uniform the density $v(\mathbf{x}, \mathbf{y})$ is, the closer is ρ to unity. The more general WW score in [13] is linked to the more general α -Chernoff divergence and its coefficient [33].

C. Sequential Weiss–Weinstein Bound

The sequential Weiss–Weinstein bound is the extension of the WW bound to a process $\mathbf{x} = \{\mathbf{x}_k\}$ with discrete time $k \in \mathbb{N}$ [22], [23]. The evolution over time is described by a state-space model

$$\mathbf{x}_{k+1} = \Phi(\mathbf{x}_k) + \mathbf{w}_k, \quad \mathbf{w}_k \sim v(\mathbf{w}_k), \quad (21a)$$

$$\mathbf{y}_k = C(\mathbf{x}_k) + \mathbf{v}_k, \quad \mathbf{v}_k \sim v(\mathbf{v}_k), \quad (21b)$$

with a mapping Φ and state noise \mathbf{w}_k . We first consider the joint WW bound for the prior and history of states $\mathbf{x}_{0:k} = [\mathbf{x}_0, \dots, \mathbf{x}_k]^T$ for deriving a recursive algorithm to iteratively compute the WW bound of every time step k . A block-diagonal matrix defines the $kN \times kN$ test point matrix

$$\mathfrak{H}_k \triangleq \begin{bmatrix} \mathbf{H}_0 & & \\ & \ddots & \\ & & \mathbf{H}_k \end{bmatrix} = [\mathfrak{h}_0, \dots, \mathfrak{h}_{kN}]. \quad (22)$$

The matrix $\mathbf{H}_\ell = [\mathbf{h}_{\ell,1}, \dots, \mathbf{h}_{\ell,N}]$ corresponds to \mathbf{H} in (17) at time ℓ . Using the error vector $\boldsymbol{\varepsilon}_{0:k} = \hat{\mathbf{x}}_{0:k}(\mathbf{y}_{1:k}) - \mathbf{x}_{0:k}$, the mean-square error matrix

$$\mathbb{E} \{ \boldsymbol{\varepsilon}_{0:k} \boldsymbol{\varepsilon}_{0:k}^T \} \succcurlyeq \mathfrak{H}_k \mathfrak{J}_k^{-1} \mathfrak{H}_k^T. \quad (23)$$

The overall matrix \mathfrak{J}_k can be partitioned into

$$\mathfrak{J}_k = \begin{bmatrix} \mathfrak{A}_{k-1} & \mathbf{0} \\ \mathbf{0} & \mathbf{B}_k^{10} & \mathbf{B}_k^{11} \end{bmatrix} \quad (24)$$

with $\mathfrak{A}_{k-1} = \text{blockdiag}(\mathbf{A}_0, \dots, \mathbf{A}_{k-1})$ and $\mathbf{0}$ is the zero-matrix of size $(k-1)N \times (k-1)N$. Matrix \mathfrak{A}_{k-1} captures information from the times $[0, k-1]$, \mathbf{B}_k^{11} the time k and $\mathbf{B}_k^{01} = (\mathbf{B}_k^{10})^T$ the transition between them. The $\mathbf{0}$ matrices in (24) are due to the Markovian property, i.e.,

$$v(\mathbf{x}_{0:k}, \mathbf{y}_{1:k}) = v(\mathbf{y}_k | \mathbf{x}_k) v(\mathbf{x}_k | \mathbf{x}_{k-1}) v(\mathbf{x}_{0:k-1}, \mathbf{y}_{1:k-1}).$$

For the time $k = 0$, we have $\mathbf{B}_0^{11} = \mathfrak{J}_0 = \mathbf{J}_0$, i.e., the bound of the prior.

In the remainder of this section, we derive a recursive update for the WW bound at time k , i.e.,

$$\mathbb{E} \{ \boldsymbol{\varepsilon}_k \boldsymbol{\varepsilon}_k^T \} \succcurlyeq \mathbf{W}_k \triangleq \mathbf{H}_k \mathbf{J}_k^{-1} \mathbf{H}_k^T. \quad (25)$$

In addition to (24), we consider the time interval $[0, k+1]$ and partition the overall matrix

$$\mathfrak{J}_{k+1} = \begin{bmatrix} \mathfrak{A}_{k-1} & \mathbf{0} & \mathbf{0} \\ \mathbf{0} & \mathbf{D}_{k+1}^{10} & \mathbf{D}_{k+1}^{11} \\ \mathbf{0} & \mathbf{0} & \mathbf{D}_{k+1}^{21} & \mathbf{D}_{k+1}^{22} \end{bmatrix}. \quad (26)$$

Matrix \mathbf{D}_{k+1}^{11} captures the time k , \mathbf{D}_{k+1}^{22} the time $k+1$ and the others the transition between the time instances. Using the Schur complement, the right lowest part of \mathfrak{J}_{k+1}^{-1} is given by the inverse of

$$\begin{aligned} \mathbf{J}_{k+1} &= \mathbf{D}_{k+1}^{22} - \begin{bmatrix} \mathbf{0} \\ \mathbf{0} \\ \mathbf{D}_{k+1}^{21} \end{bmatrix}^T \begin{bmatrix} \mathfrak{A}_{k-1} & \mathbf{0} \\ \mathbf{0} & \mathbf{D}_k^{10} & \mathbf{D}_k^{11} \end{bmatrix}^{-1} \begin{bmatrix} \mathbf{0} \\ \mathbf{0} \\ \mathbf{D}_{k+1}^{12} \end{bmatrix} \\ &= \mathbf{D}_{k+1}^{22} - \mathbf{D}_{k+1}^{21} \underbrace{\left(\mathbf{D}_{k+1}^{11} - \mathbf{D}_{k+1}^{10} \mathbf{A}_{k-1}^{-1} \mathbf{D}_{k+1}^{01} \right)^{-1}}_{\triangleq \mathbf{A}_k} \mathbf{D}_{k+1}^{12}. \end{aligned} \quad (27)$$

We compare it with

$$\mathbf{J}_k = \mathbf{D}_k^{22} - \mathbf{D}_k^{21} \mathbf{A}_{k-1}^{-1} \mathbf{D}_k^{12}. \quad (28)$$

The sequential update becomes

$$\mathbf{A}_k = \mathbf{D}_{k+1}^{11} - \mathbf{D}_{k+1}^{10} \mathbf{A}_{k-1}^{-1} \mathbf{D}_{k+1}^{01}, \quad (29a)$$

$$\mathbf{J}_{k+1} = \mathbf{D}_{k+1}^{22} - \mathbf{D}_{k+1}^{21} \mathbf{A}_k^{-1} \mathbf{D}_{k+1}^{12}, \quad (29b)$$

for all $k = 0, 1, \dots$. Matrix $\mathbf{A}_{-1}^{-1} := \mathbf{0}$ whereas \mathbf{J}_0^{-1} is set to the co-variance of the prior. According to (19) and (26),

$$[\mathbf{D}_{k+1}^{ij}]_{mn} = 2 \frac{e^{\mu_1} - e^{\mu_2}}{e^{\mu_3} e^{\mu_4}}, \quad i, j \in \{0, 1, 2\}, \quad (29c)$$

with

$$\mu_1 = \mu(\mathfrak{h}_{(k-2+i)N+m}, -\mathfrak{h}_{(k-2+j)N+n}), \quad (29d)$$

$$\mu_2 = \mu(\mathfrak{h}_{(k-2+i)N+m}, \mathfrak{h}_{(k-2+j)N+n}), \quad (29e)$$

$$\mu_3 = \mu(\mathfrak{h}_{(k-2+i)N+m}, \mathbf{0}), \quad (29f)$$

$$\mu_4 = \mu(\mathbf{0}, \mathfrak{h}_{(k-2+j)N+n}), \quad (29g)$$

and (29h) at the bottom of the page with

$$v(\mathbf{y}_0 | \mathbf{x}_0) v(\mathbf{x}_0 | \mathbf{x}_{-1}) := v(\mathbf{y}_0) v(\mathbf{x}_0). \quad (29i)$$

In contrast to [22], we use Expectation (1) in (29h) and this entails an additional density in the denominator.

Inspecting (29h) and (26) leads to Proposition 1.

Proposition 1: Given a time-invariant state-space model with time-invariant noise distributions and sub-matrices $\mathbf{H}_k := \mathbf{H}_0$. Then $\mathbf{D}_k^{10} = \mathbf{D}_k^{21}$ and $\mathbf{D}_k^{01} = \mathbf{D}_k^{12} = (\mathbf{D}_k^{21})^T$ for $k > 2$.

$$\mu(\mathfrak{h}_a, \mathfrak{h}_b) = \ln \mathbb{E} \left\{ \frac{\prod_{\ell=0}^{k+1} v(\mathbf{y}_\ell | \mathbf{x}_\ell + \mathbf{h}_{\ell,a})^{1/2} v(\mathbf{x}_\ell + \mathbf{h}_{\ell,a} | \mathbf{x}_{\ell-1} + \mathbf{h}_{\ell-1,a})^{1/2} v(\mathbf{y}_\ell | \mathbf{x}_\ell - \mathbf{h}_{\ell,b})^{1/2} v(\mathbf{x}_\ell - \mathbf{h}_{\ell,b} | \mathbf{x}_{\ell-1} - \mathbf{h}_{\ell-1,b})^{1/2}}{v(\mathbf{x}_{0:k+1}, \mathbf{y}_{1:k+1})} \right\} \quad (29h)$$

D. Linear Models

We condense, reformulate, and expand Assumption 1, Class 1, and Lemma 5 of [22]. This enables Section III to draw on the following lemmas. We further utilize Expectation (1) and finally approach linear models.

Lemma 2: If the expectation in (29h) can be factored into independent expectations, i.e.,

$$\mu(\mathbf{h}_a, \mathbf{h}_b) = \ln(E_0 \cdots E_{k+1}) \quad (30)$$

where

$$E_\ell \triangleq \mathbb{E} \left\{ \frac{v(\mathbf{y}_\ell | \mathbf{x}_\ell + \mathbf{h}_{\ell,a})^{1/2} v(\mathbf{y}_\ell | \mathbf{x}_\ell - \mathbf{h}_{\ell,b})^{1/2}}{v(\mathbf{y}_\ell | \mathbf{x}_\ell)} \times \frac{v(\mathbf{x}_\ell + \mathbf{h}_{\ell,a} | \mathbf{x}_{\ell-1} + \mathbf{h}_{\ell-1,a})^{1/2}}{v(\mathbf{x}_\ell | \mathbf{x}_{\ell-1})} \times v(\mathbf{x}_\ell - \mathbf{h}_{\ell,b} | \mathbf{x}_{\ell-1} - \mathbf{h}_{\ell-1,b})^{1/2} \right\} \quad (31)$$

then

$$\mathbf{D}_{k+1}^{01} = (\mathbf{D}_{k+1}^{10})^\top = \mathbf{B}_k^{01} = (\mathbf{B}_k^{10})^\top. \quad (32)$$

Proof: Let us focus on (29h). We first recast (29h) as (33) and omit all zero vectors $\mathbf{h}_{\ell,a}$ and $\mathbf{h}_{\ell,b}$. To compute \mathbf{B}_k , Part (33a) and (33b) at the bottom of the page, are separable. Part (33a) is an expectation $E_{k+1}(\mathbf{h}_{k,a}) = E_{k+1}(\mathbf{0}) = 1$. To compute \mathbf{D}_{k+1}^{10} and \mathbf{D}_{k+1}^{01} we assume independent expectations (30). Thus, Part (33a) and Part (33b) are also separable. Part (33a) is an expectation $E_{k+1}(\mathbf{h}_{k,a})$. For $\mu(\mathbf{0}, \mathbf{h}_b)$ in (29h), the expectation $E_{k+1}(\mathbf{h}_{k,a}) = E_{k+1}(\mathbf{0}) = 1$. For $\mu(\mathbf{h}_a, -\mathbf{h}_b)$, $\mu(\mathbf{h}_a, \mathbf{h}_b)$, and $\mu(\mathbf{h}_a, \mathbf{0})$, the expectations $E_{k+1}(\mathbf{h}_{k,a})$ are equal. Thus the $E_{k+1}(\mathbf{h}_{k,a})$ cancels in (29h). What remains is identical to \mathbf{B}_k^{01} . ■

Lemma 3 (Linear Transition Equation): Given a linear state-transition equation

$$\mathbf{x}_{k+1} = \Phi \mathbf{x}_k + \mathbf{w}_k, \quad \mathbf{w}_k \sim v(\mathbf{w}_k). \quad (34)$$

Then the conditions for (30) are fulfilled.

Proof: Integrating over the transition densities (as in (1))

$$\begin{aligned} & \int \frac{v(\mathbf{x}_\ell + \mathbf{h}_{\ell,a} | \mathbf{x}_{\ell-1} + \mathbf{h}_{\ell-1,a})^{1/2}}{v(\mathbf{x}_\ell | \mathbf{x}_{\ell-1})} \\ & \times v(\mathbf{x}_\ell - \mathbf{h}_{\ell,b} | \mathbf{x}_{\ell-1} - \mathbf{h}_{\ell-1,b})^{1/2} dP_{\mathbf{x}_\ell | \mathbf{x}_{\ell-1}} \\ & = \int \frac{v_{\mathbf{w}_\ell}(\mathbf{w}_\ell + \mathbf{h}_{\ell,a} - \Phi \mathbf{h}_{\ell-1,a})^{1/2}}{v_{\mathbf{w}_\ell}(\mathbf{w}_\ell)} \\ & \times v_{\mathbf{w}_\ell}(\mathbf{w}_\ell - \mathbf{h}_{\ell,b} + \Phi \mathbf{h}_{\ell-1,b})^{1/2} dP_{\mathbf{w}_\ell} \end{aligned} \quad (35)$$

with $\mathbf{w}_\ell = \mathbf{x}_\ell - \Phi \mathbf{x}_{\ell-1}$ and the conditional probability measure $P_{\mathbf{x}_\ell | \mathbf{x}_{\ell-1}}$. Observe that (35) is independent of time $\ell - 1$. ■

Additionally to the transition equation in Lemma 3, we address the measurement equation.

Corollary 4 (Linear Measurement Equation): Given the linear transition equation (34) and the measurement equation

$$\mathbf{y}_k = \mathbf{C}_k \mathbf{x}_k + \mathbf{v}_k, \quad \mathbf{v}_k \sim v(\mathbf{v}_k). \quad (36)$$

Let the state and measurement noise be independent.

Then

$$\mu(\mathbf{h}_a, \mathbf{h}_b) = \ln(E_0 \cdots E_{k+1} E'_0 \cdots E'_{k+1}), \quad (37)$$

with

$$E_\ell \triangleq \mathbb{E} \left\{ \frac{v(\mathbf{x}_\ell + \mathbf{h}_{\ell,a} | \mathbf{x}_{\ell-1} + \mathbf{h}_{\ell-1,a})^{1/2}}{v(\mathbf{x}_\ell | \mathbf{x}_{\ell-1})} \times v(\mathbf{x}_\ell - \mathbf{h}_{\ell,b} | \mathbf{x}_{\ell-1} - \mathbf{h}_{\ell-1,b})^{1/2} \right\}, \quad (38a)$$

$$E'_\ell \triangleq \mathbb{E} \left\{ \frac{v(\mathbf{y}_\ell | \mathbf{x}_\ell + \mathbf{h}_{\ell,a})^{1/2} v(\mathbf{y}_\ell | \mathbf{x}_\ell - \mathbf{h}_{\ell,b})^{1/2}}{v(\mathbf{y}_\ell | \mathbf{x}_\ell)} \right\}, \quad (38b)$$

i.e., the expectation over $\mathbf{x}_{0:k+1}, \mathbf{y}_{1:k+1}$ splits into expectations w.r.t. $\mathbf{x}_\ell, \mathbf{y}_\ell$.

Proof: The factorization corresponding to the transition densities have been proved with Lemma 2. Dually, the factorization of the integrals concerning the measurement noise are proved in the following.

Due to the additivity of the measurement function,

$$\begin{aligned} & \int \frac{v(\mathbf{y}_\ell | \mathbf{x}_\ell + \mathbf{h}_{\ell,a})^{1/2} v(\mathbf{y}_\ell | \mathbf{x}_\ell - \mathbf{h}_{\ell,b})^{1/2}}{v(\mathbf{y}_\ell | \mathbf{x}_\ell)} dP_{\mathbf{y}_\ell | \mathbf{x}_\ell} \\ & = \int \frac{v_{\mathbf{v}_\ell}(\mathbf{v}_\ell - \mathbf{C}_\ell \mathbf{h}_{\ell,a})^{1/2} v_{\mathbf{v}_\ell}(\mathbf{v}_\ell + \mathbf{C}_\ell \mathbf{h}_{\ell,b})^{1/2}}{v_{\mathbf{v}_\ell}(\mathbf{v}_\ell)} dP_{\mathbf{v}_\ell} \end{aligned} \quad (39)$$

with $\mathbf{v}_\ell = \mathbf{y}_\ell - \mathbf{C}_\ell \mathbf{x}_\ell$.

Due to the independence of \mathbf{v}_ℓ and \mathbf{w}_ℓ and their independence from time $\ell - 1$, (33) is separable into factors due to innovation and measurement noise. ■

Next we assume independence between continuous and discrete random sub-vectors of the innovation noise vector, say

$$v(\mathbf{w}_k^c, \mathbf{w}_k^d) = f(\mathbf{w}_k^c) p(\mathbf{w}_k^d). \quad (40)$$

$$\mu(\mathbf{h}_a, \mathbf{h}_b) = \ln \mathbb{E} \left\{ \frac{v(\mathbf{x}_{k+1} | \mathbf{x}_k + \mathbf{h}_{k,a})^{1/2} v(\mathbf{x}_{k+1} | \mathbf{x}_k)^{1/2}}{v(\mathbf{x}_{k+1} | \mathbf{x}_k)} \right. \quad (33a)$$

$$\times \frac{v(\mathbf{y}_k | \mathbf{x}_k + \mathbf{h}_{k,a})^{1/2} v(\mathbf{y}_k | \mathbf{x}_k)^{1/2} v(\mathbf{x}_k + \mathbf{h}_{k,a} | \mathbf{x}_{k-1})^{1/2} v(\mathbf{x}_k | \mathbf{x}_{k-1} - \mathbf{h}_{k-1,b})^{1/2}}{v(\mathbf{y}_k | \mathbf{x}_k) v(\mathbf{x}_k | \mathbf{x}_{k-1})} \quad (33b)$$

$$\left. \times \frac{v(\mathbf{y}_{k-1} | \mathbf{x}_{k-1})^{1/2} v(\mathbf{y}_{k-1} | \mathbf{x}_{k-1} - \mathbf{h}_{k-1,b})^{1/2} v(\mathbf{x}_{k-1} | \mathbf{x}_{k-2})^{1/2} v(\mathbf{x}_{k-1} - \mathbf{h}_{k-1,b} | \mathbf{x}_{k-2})^{1/2}}{v(\mathbf{y}_{k-1} | \mathbf{x}_{k-1}) v(\mathbf{x}_{k-1} | \mathbf{x}_{k-2})} \frac{v(\mathbf{x}_{0:k-2}, \mathbf{y}_{1:k-2})}{v(\mathbf{x}_{0:k-2}, \mathbf{y}_{1:k-2})} \right\}.$$

Corollary 5: With (34), (36), and (40), Equation (37) factorizes further into

$\mu(\mathbf{h}_a, \mathbf{h}_b) = \ln(E_0^c \cdots E_{k+1}^c E_0^d \cdots E_{k+1}^d E_0' \cdots E_{k+1}')$, (41) where E^c denotes the expectation over continuous probability distributions whereas E^d denotes the expectation over discrete ones.

In the remainder of our paper, we compute the expectations in (41) for different noise and priors.

E. Sequential WW Bound for the Linear Transition Model

Recursion (29) simplifies if the transition function $\Phi = \mathbf{\Phi}$ is linear. Applying the matrix inversion lemma to (24) gives

$$\mathbf{J}_k = \mathbf{B}_k^{11} - \mathbf{B}_k^{10} \mathbf{A}_k^{-1} \mathbf{B}_k^{01}. \quad (42)$$

Substitution of (42) and (32) into (27) leads to

$$\boxed{\mathbf{J}_{k+1} = \mathbf{D}_{k+1}^{22} - \mathbf{D}_{k+1}^{21} (\mathbf{D}_{k+1}^{11} + \mathbf{J}_k - \mathbf{B}_k^{11})^{-1} \mathbf{D}_{k+1}^{12}} \quad (43)$$

with $\mathbf{B}_0^{11} = \mathbf{J}_0$ and $\mathbf{B}_k^{11} = \mathbf{D}_k^{22}$, $k = 1, 2, \dots$ [22].

III. MODELS

In the remainder, we use Corollary 4 and 5 to derive analytic SWW bounds for different noise and prior. The solutions are general in the sense that the structure is the same for different distributions. Furthermore, we investigate the SWW bound for the case of states and noise quantized uniformly from continuous distributions. We prove that SWW bounds of continuous and uniformly quantized states are equal for suitable choices of \mathfrak{H}_k . We assume uniform quantization with step size $\Delta_{\mathbf{x}}$, i.e., $\mathbf{x}_k^d / \Delta_{\mathbf{x}} \in \mathbb{Z}^N$ and the probability densities are sampled and normalized.

Similar to the continuous linear state-space model (34) and (36), we define the *discrete model*

$$\mathbf{x}_{k+1}^d = \mathbf{\Phi} \mathbf{x}_k^d + \mathbf{w}_k^d, \quad \mathbf{x}_k^d \in \mathbb{R}^N, \quad (44a)$$

$$\mathbf{y}_k = \mathbf{C} \mathbf{x}_k^d + \mathbf{v}_k, \quad (44b)$$

$$\mathbf{w}_k^d \sim \frac{1}{c''} f_{\mathbf{w}_k}(\mathbf{w}_k^d), \quad \mathbf{x}_0^d \sim \frac{1}{c'''} f_{\mathbf{x}_0}(\mathbf{x}_0^d), \quad (44c)$$

and the *hybrid model*

$$\begin{aligned} \mathbf{x}_{k+1}^c &= \mathbf{\Phi}^c \mathbf{x}_k^c + \mathbf{\Phi}^{cd} \mathbf{x}_k^d + \mathbf{w}_k^c, & \mathbf{x}_k^c &\in \mathbb{R}^{N^c}, \\ \mathbf{x}_{k+1}^d &= \mathbf{\Phi}^d \mathbf{x}_k^d + \mathbf{w}_k^d, & \mathbf{x}_k^d &\in \mathbb{R}^{N^d}, \\ \mathbf{y}_k &= \mathbf{C}^c \mathbf{x}_k^c + \mathbf{C}^d \mathbf{x}_k^d + \mathbf{v}_k, \\ \mathbf{w}_k^c &\sim f(\mathbf{w}_k^c), \quad \mathbf{x}_0^c \sim f(\mathbf{x}_0^c), & \mathbf{v}_k &\sim f_{\mathbf{v}_k}(\mathbf{v}_k), \\ \mathbf{w}_k^d &\sim \frac{1}{c''} f_{\mathbf{w}_k}(\mathbf{w}_k^d), & \mathbf{x}_0^d &\sim \frac{1}{c'''} f_{\mathbf{x}_0}(\mathbf{x}_0^d), \end{aligned} \quad (45)$$

where $f_{\mathbf{x}_0^c}$, $f_{\mathbf{w}_k^c}$ and $f_{\mathbf{v}_k}$ are PDFs of interest. Factors c'' and c''' normalize the densities. Variable $N = N^c + N^d$ is the number of states.

IV. ANALYTIC SOLUTION FOR GAUSSIAN NOISE/PRIOR

In this section we derive lower bounds for Gaussian [34] noise and priors $\mathcal{N}\{\mathbf{m}_{\mathbf{x}_k}, \mathbf{C}_{\mathbf{x}_k}\}$, i.e.,

$$v(\mathbf{x}_k) \triangleq \frac{1}{(2\pi)^{N/2} (\det \mathbf{C}_{\mathbf{x}_k})^{1/2}} e^{-\frac{1}{2} \|\mathbf{x}_k - \mathbf{m}_{\mathbf{x}_k}\|_{\mathbf{C}_{\mathbf{x}_k}^{-1}}^2} \quad (46)$$

with the mean $\mathbf{m}_{\mathbf{x}_k}$, the covariance matrix $\mathbf{C}_{\mathbf{x}_k}$, and the weighted norm $\|\mathbf{h}\|_{\mathbf{C}_{\mathbf{x}}^{-1}} \triangleq (\mathbf{h}^T \mathbf{C}_{\mathbf{x}}^{-1} \mathbf{h})^{1/2}$. For this case, we use the Bayesian Bhattacharyya coefficient (20)

$$\rho_{\mathbf{x}}^G(\mathbf{h}) \triangleq e^{-\frac{1}{8} \|\mathbf{h}\|_{\mathbf{C}_{\mathbf{x}}^{-1}}^2}. \quad (47)$$

For discretized Gaussian densities, $\mathbf{h} / \Delta_{\mathbf{x}} \in \mathbb{Z}^N$. We make extensive use of Lemmas formulated in the Appendix A.

Theorem 6 (SWW Bound/Gaussian Distributions): Consider a linear continuous, discrete, or hybrid state-space model. Let the prior, the innovation noise, and the likelihood function be Gaussian and statistically independent. Then the SWW lower bound (25) for $k \in \mathbb{N}$ is computed by (43) with (50) at the bottom of the page, with $\rho(\mathbf{h}) := \rho^G(\mathbf{h})$, which corresponds to

$$\begin{aligned} [\mathbf{D}_{k+1}^{11}]_{a,b} &= 4 \sinh \left[\frac{1}{4} \mathbf{h}_{k,a}^T \left(\mathbf{\Phi}^T \mathbf{C}_{\mathbf{w}_k}^{-1} \mathbf{\Phi} \right. \right. \\ &\quad \left. \left. + \mathbf{C}^T \mathbf{C}_{\mathbf{v}_k}^{-1} \mathbf{C} + \mathbf{C}_{\mathbf{w}_{k-1}}^{-1} \right) \mathbf{h}_{k,b} \right], \end{aligned} \quad (48a)$$

$$[\mathbf{D}_{k+1}^{12}]_{a,b} = -4 \sinh \left[\frac{1}{4} \mathbf{h}_{k,a}^T \mathbf{\Phi}^T \mathbf{C}_{\mathbf{w}_k}^{-1} \mathbf{h}_{k+1,b} \right] = [\mathbf{D}_{k+1}^{21}]_{b,a}, \quad (48b)$$

$$[\mathbf{D}_{k+1}^{22}]_{a,b} = 4 \sinh \left[\frac{1}{4} \mathbf{h}_{k+1,a}^T \left(\mathbf{C}^T \mathbf{C}_{\mathbf{v}_{k+1}}^{-1} \mathbf{C} + \mathbf{C}_{\mathbf{w}_k}^{-1} \right) \mathbf{h}_{k+1,b} \right]. \quad (48c)$$

$$\begin{aligned} [\mathbf{D}_{k+1}^{11}]_{a,b} &= 2 \left(\rho_{\mathbf{w}_k}(\mathbf{\Phi} \mathbf{h}_{k,a} - \mathbf{\Phi} \mathbf{h}_{k,b}) \rho_{\mathbf{v}_k}(\mathbf{C} \mathbf{h}_{k,a} - \mathbf{C} \mathbf{h}_{k,b}) \rho_{\mathbf{w}_{k-1}}(\mathbf{h}_{k,a} - \mathbf{h}_{k,b}) \right. \\ &\quad \left. - \rho_{\mathbf{w}_k}(\mathbf{\Phi} \mathbf{h}_{k,a} + \mathbf{\Phi} \mathbf{h}_{k,b}) \rho_{\mathbf{v}_k}(\mathbf{C} \mathbf{h}_{k,a} + \mathbf{C} \mathbf{h}_{k,b}) \rho_{\mathbf{w}_{k-1}}(\mathbf{h}_{k,a} + \mathbf{h}_{k,b}) \right) \\ &\quad / \left(\rho_{\mathbf{w}_k}(\mathbf{\Phi} \mathbf{h}_{k,a}) \rho_{\mathbf{v}_k}(\mathbf{C} \mathbf{h}_{k,a}) \rho_{\mathbf{w}_{k-1}}(\mathbf{h}_{k,a}) \rho_{\mathbf{w}_k}(\mathbf{\Phi} \mathbf{h}_{k,b}) \rho_{\mathbf{v}_k}(\mathbf{C} \mathbf{h}_{k,b}) \rho_{\mathbf{w}_{k-1}}(\mathbf{h}_{k,b}) \right) \\ [\mathbf{D}_{k+1}^{12}]_{a,b} &= [\mathbf{D}_{k+1}^{21}]_{b,a} = 2 \frac{\rho_{\mathbf{w}_k}(\mathbf{\Phi} \mathbf{h}_{k,a} + \mathbf{h}_{k+1,b}) - \rho_{\mathbf{w}_k}(\mathbf{\Phi} \mathbf{h}_{k,a} - \mathbf{h}_{k+1,b})}{\rho_{\mathbf{w}_k}(\mathbf{\Phi} \mathbf{h}_{k,a}) \rho_{\mathbf{w}_k}(\mathbf{h}_{k+1,b})} \\ [\mathbf{D}_{k+1}^{22}]_{a,b} &= 2 \left(\rho_{\mathbf{v}_{k+1}}(\mathbf{C} \mathbf{h}_{k+1,a} - \mathbf{C} \mathbf{h}_{k+1,b}) \rho_{\mathbf{w}_k}(\mathbf{h}_{k+1,a} - \mathbf{h}_{k+1,b}) \right. \\ &\quad \left. - \rho_{\mathbf{v}_{k+1}}(\mathbf{C} \mathbf{h}_{k+1,a} + \mathbf{C} \mathbf{h}_{k+1,b}) \rho_{\mathbf{w}_k}(\mathbf{h}_{k+1,a} + \mathbf{h}_{k+1,b}) \right) \\ &\quad / \left(\rho_{\mathbf{v}_{k+1}}(\mathbf{C} \mathbf{h}_{k+1,a}) \rho_{\mathbf{w}_k}(\mathbf{h}_{k+1,a}) \rho_{\mathbf{v}_{k+1}}(\mathbf{C} \mathbf{h}_{k+1,b}) \rho_{\mathbf{w}_k}(\mathbf{h}_{k+1,b}) \right) \end{aligned} \quad (50)$$

For the initial $k = 0$, matrix \mathbf{D}_1^{11} for (43) is given by (51), shown at the bottom of the page, with $\rho_{\mathbf{x}_0}(\mathbf{h}) := \rho_{\mathbf{x}_0}^G(\mathbf{h})$, i.e.,

$$[\mathbf{D}_1^{11}]_{a,b} = 4 \sinh \left[\frac{1}{4} \mathbf{h}_{0,a}^T \left(\Phi^T \mathbf{C}_{\mathbf{w}_0}^{-1} \Phi + \mathbf{C}_{\mathbf{x}_0}^{-1} \right) \mathbf{h}_{0,b} \right]. \quad (49)$$

Proof: First, the semi-invariant BD (29c) is re-cast into (29h). According to (22), $\mathbf{h}_{\ell,a} = 0$ if $a < \ell N$ and $a > (\ell + 1)N$. Thus we may remove them from (29h). Due to linearity we invoke Corollary 4. We apply successively Lemmas 14, 15, and 16. Together with (47), we get the analytic solution of the BD. Inserting this four-times into (29c) gives us one element of \mathbf{D}_{k+1}^{12} .

Further details for $k > 0$ are given in (52), shown at the bottom of the page. There the BD for the elements of \mathbf{D}_{k+1}^{12} is derived. From the beginning we consider the existence of a PD, either PDF or PMF. This gives the first two lines in (52). Finally, we insert the last line four times into (29c).

For $k = 0$ we use the fact that $v(\mathbf{y}_0|\mathbf{x}_0) := v_{\mathbf{y}_0}(\mathbf{y}_0)$, and $v(\mathbf{x}_0|\mathbf{x}_{-1}) := v(\mathbf{x}_0)$. The main difference to $k > 0$ is the equality

$$\int v_{\mathbf{x}_0}(\mathbf{x}_0 + \mathbf{h}_{0,a})^{1/2} v_{\mathbf{x}_0}(\mathbf{x}_0 - \mathbf{h}_{0,b})^{1/2} d\lambda_{\mathbf{x}_0} = \rho_{\mathbf{x}_0}^G(\mathbf{h}_{0,a} + \mathbf{h}_{0,b}). \quad (53)$$

Inserting (47) into (50) gives (48). ■

Observe that the hybrid and discretized models assume that $c_1, c_2 \in \{0, 1\}$ in (2), i.e., the densities are either continuous or discrete. For hybrid densities with $c_1, c_2 \in (0, 1)$ and due to (3), the integrals split into discrete and continuous parts.

In the next sections, we observe that the structure of (43), (50) and (51) is similar for other distributions. Hence, (50) is discussed in detail.

Let us compare ρ^G with (8) and (60) in [32], where we set $p_1(x)$ to Gaussian $\mathcal{N}\{\mathbf{0}, \mathbf{C}_{\mathbf{x}}\}$ and $p_2(x)$ to $\mathcal{N}\{\mathbf{h}, \mathbf{C}_{\mathbf{x}}\}$. This shows that Function ρ^G is the Bhattacharyya coefficient

$\rho \in [0, 1]$. In (50), ρ quantifies the non-constancy of the densities. The sharper a density is, the lower ρ is.

We observe that the structure of (50) stems from (29c). Matrix \mathbf{D}_{k+1}^{11} reflects the influence of innovation and measurement noise at time k on $k+1$. Therefore, transition matrix Φ and measurement matrix \mathbf{C} arise. Matrix $\mathbf{D}_{k+1}^{12} = (\mathbf{D}_{k+1}^{21})^T$ addresses the transition between k and $k+1$. Thus, it is independent of the measurements and there is no function $\rho_{\mathbf{v}_k}$. Matrix \mathbf{D}_{k+1}^{22} addresses only time $k+1$. The structure is the same as of \mathbf{D}_{k+1}^{11} except that no $\rho_{\mathbf{w}_{k+1}}$ occurs due to causality.

For Gaussian densities, (50) becomes (48). For small \mathbf{h} -vectors, $\sinh(x) \approx x$. Thus we get

$$[\mathbf{D}_{k+1}^{22}]_{a,b} = \mathbf{h}_{k+1,a}^T \left(\mathbf{C}^T \mathbf{C}_{\mathbf{v}_{k+1}}^{-1} \mathbf{C} + \mathbf{C}_{\mathbf{w}_k}^{-1} \right) \mathbf{h}_{k+1,b}. \quad (54a)$$

It represents the influence of noise on the SWW bound at time $k+1$, hence vectors $\mathbf{h}_{k+1,a}$ and $\mathbf{h}_{k+1,b}$ affect the bound due to measurement noise at $k+1$ and transition noise at k (cf. equation (34)). The transition between k and $k+1$ is represented by

$$[\mathbf{D}_{k+1}^{12}]_{a,b} = -\mathbf{h}_{k,a}^T \Phi^T \mathbf{C}_{\mathbf{w}_k}^{-1} \mathbf{h}_{k+1,b} = [\mathbf{D}_{k+1}^{21}]_{b,a} \quad (54b)$$

and hence the bound is affected by transition noise at k , i.e., $\Phi \mathbf{h}_{k,a}$ and $\mathbf{h}_{k+1,b}$ perturb the matrix. Eventually,

$$[\mathbf{D}_{k+1}^{11}]_{a,b} = \mathbf{h}_{k,a}^T \left(\Phi^T \mathbf{C}_{\mathbf{w}_k}^{-1} \Phi + \mathbf{C}^T \mathbf{C}_{\mathbf{v}_k}^{-1} \mathbf{C} + \mathbf{C}_{\mathbf{w}_{k-1}}^{-1} \right) \mathbf{h}_{k,b}, \quad (54c)$$

represents the noise at time k affecting time $k+1$. This includes measurement noise at k and transition noise at $k-1$ and k .

Note that the higher the variance of a Gaussian distribution, the flatter its density. In (54), the higher the variances, the smaller the \mathbf{D} -matrices. Smaller \mathbf{D} -matrices tends to give a smaller \mathbf{J}_k . This gives an increased bound (25).

Under one condition, the SWW bound for the continuous, the discretized, and the hybrid models are equal:

$$[\mathbf{D}_1^{11}]_{a,b} = 2 \frac{\rho_{\mathbf{w}_0}(\Phi \mathbf{h}_{0,a} - \Phi \mathbf{h}_{0,b}) \rho_{\mathbf{x}_0}(\mathbf{h}_{0,a} - \mathbf{h}_{0,b}) - \rho_{\mathbf{w}_0}(\Phi \mathbf{h}_{0,a} + \Phi \mathbf{h}_{0,b}) \rho_{\mathbf{x}_0}(\mathbf{h}_{0,a} + \mathbf{h}_{0,b})}{\rho_{\mathbf{w}_0}(\Phi \mathbf{h}_{0,a}) \rho_{\mathbf{x}_0}(\mathbf{h}_{0,a}) \rho_{\mathbf{w}_0}(\Phi \mathbf{h}_{0,b}) \rho_{\mathbf{x}_0}(\mathbf{h}_{0,b})} \quad (51)$$

$$\begin{aligned} \mathbf{D}_{k+1}^{12} : \mu(\mathbf{h}_a, \mathbf{h}_b) &= \ln \int \int f(\mathbf{y}_{k+1}|\mathbf{x}_{k+1})^{1/2} f(\mathbf{x}_{k+1}|\mathbf{x}_k + \mathbf{h}_{k,a})^{1/2} f(\mathbf{y}_k|\mathbf{x}_k + \mathbf{h}_{k,a})^{1/2} f(\mathbf{x}_k + \mathbf{h}_{k,a}|\mathbf{x}_{k-1})^{1/2} \\ &\quad \times f(\mathbf{y}_{k+1}|\mathbf{x}_{k+1} - \mathbf{h}_{k+1,b})^{1/2} f(\mathbf{x}_{k+1} - \mathbf{h}_{k+1,b}|\mathbf{x}_k)^{1/2} f(\mathbf{y}_k|\mathbf{x}_k)^{1/2} f(\mathbf{x}_k|\mathbf{x}_{k-1})^{1/2} d\lambda_{\mathbf{x}_{k:k+1}} d\lambda_{\mathbf{y}_{k:k+1}} \\ &\stackrel{\text{Corollary 4}}{=} \ln \int \int \int \int f_{\mathbf{v}_{k+1}}(\mathbf{y}_{k+1} - \mathbf{C}\mathbf{x}_{k+1})^{1/2} f_{\mathbf{v}_{k+1}}(\mathbf{y}_{k+1} - \mathbf{C}(\mathbf{x}_{k+1} - \mathbf{h}_{k+1,b}))^{1/2} d\lambda_{\mathbf{y}_{k+1}} \\ &\quad \times f_{\mathbf{w}_k}(\mathbf{x}_{k+1} - \Phi(\mathbf{x}_k + \mathbf{h}_{k,a}))^{1/2} f_{\mathbf{w}_k}(\mathbf{x}_{k+1} - \mathbf{h}_{k+1,b} - \Phi\mathbf{x}_k)^{1/2} d\lambda_{\mathbf{x}_{k+1}} \\ &\quad \times f_{\mathbf{v}_k}(\mathbf{y}_k - \mathbf{C}(\mathbf{x}_k + \mathbf{h}_{k,a}))^{1/2} f_{\mathbf{v}_k}(\mathbf{y}_k - \mathbf{C}\mathbf{x}_k)^{1/2} d\lambda_{\mathbf{y}_k} \\ &\quad \times f_{\mathbf{w}_{k-1}}(\mathbf{x}_k + \mathbf{h}_{k,a} - \Phi\mathbf{x}_{k-1})^{1/2} f_{\mathbf{w}_{k-1}}(\mathbf{x}_k - \Phi\mathbf{x}_{k-1})^{1/2} d\lambda_{\mathbf{x}_k} \\ &\stackrel{\text{Lemma 14 \& 16}}{=} \ln \rho_{\mathbf{v}_{k+1}}(\mathbf{C}\mathbf{h}_{k+1,b}) \rho_{\mathbf{w}_k}(\Phi \mathbf{h}_{k,a} - \mathbf{h}_{k+1,b}) \rho_{\mathbf{v}_k}(\mathbf{C}\mathbf{h}_{k,a}) \rho_{\mathbf{w}_{k-1}}(\mathbf{h}_{k,a}). \end{aligned}$$

Proposition 7 (Equality of Bounds): Given the continuous model (34), the discrete model (44), and the hybrid model (45). Let all distributions be either continuous or discretized Gaussian. If

$$\mathfrak{H}_k / \Delta_{\mathbf{x}} \in \mathbb{Z}^{KN \times KN} \quad (55)$$

then the SWW bound of all three models are equal.

Proof: Consider the proof of Theorem 6. First, we address the prior. We compare the integral with respect to the Lebesgue measure for the continuous model with the integral with respect to the counting measure for discretized and hybrid models. Let $\mathfrak{H}_k^d \in \mathbb{Z}^{KN \times KN}$. If

$$\mathfrak{H}_k = \Delta_{\mathbf{x}} \mathfrak{H}_k^d \quad (56)$$

then

$$\rho_{\mathbf{x}_0}^G(\mathbf{h}_{0,a} + \mathbf{h}_{0,b}) = \rho_{\mathbf{x}_0}^G(\Delta_{\mathbf{x}} \mathbf{h}_{0,a}^d + \Delta_{\mathbf{x}} \mathbf{h}_{0,b}^d).$$

Next we consider the innovation noise. Inspecting Lemma 14 gives

$$\begin{aligned} & \rho_{\mathbf{w}_k}^G(\mathbf{h}_{k+1,a} - \Phi \mathbf{h}_{k,a} + \mathbf{h}_{k+1,b} - \Phi \mathbf{h}_{k,b}) \\ &= \rho_{\mathbf{w}_k}^G(\Delta_{\mathbf{x}}(\mathbf{h}_{k+1,a}^d - \Phi \mathbf{h}_{k,a}^d + \mathbf{h}_{k+1,b}^d - \Phi \mathbf{h}_{k,b}^d)) \end{aligned} \quad (57)$$

and this leads to $\mathbf{D}_1^{11,c} = \mathbf{D}_1^{11,d}$ (cf. Equation (51)). Additionally, inspecting Lemma 16 gives

$$\begin{aligned} & \rho_{\mathbf{v}_k}^G(-\mathbf{C}\mathbf{h}_{k+1,a} - \mathbf{C}\mathbf{h}_{k+1,b}) \\ &= \rho_{\mathbf{v}_k}^G(\Delta_{\mathbf{x}}(-\mathbf{C}\mathbf{h}_{k+1,a}^d - \mathbf{C}\mathbf{h}_{k+1,b}^d)). \end{aligned} \quad (58)$$

The \mathbf{D}_k^{ij} -matrices become equal for all three models. \blacksquare

V. ANALYTIC SOLUTION FOR UNIFORM DISTRIBUTIONS

Similar to previous section, we now provide the analytic SWW bound for multivariate independent uniform densities $\text{Unif}\{\mathbf{r}_k, \mathbf{s}_k\}$ [34], i.e.,

$$v(\mathbf{x}_k) \triangleq \prod_{\ell=1}^N \frac{1}{[\mathbf{s}_k - \mathbf{r}_k]_{\ell}} \mathbb{1}_{[\mathbf{x}_k]_{\ell} \geq [\mathbf{r}_k]_{\ell}, [\mathbf{x}_k]_{\ell} \leq [\mathbf{s}_k]_{\ell}} \quad (59)$$

with indicator function $\mathbb{1}$. We utilize

$$\rho_{\mathbf{x}_k}^U(\mathbf{h}) \triangleq \prod_{\ell=1}^N \begin{cases} \left[1 - \frac{|\mathbf{h}_{\ell}|}{[\mathbf{s}_{\mathbf{x}_k}]_{\ell}}\right], & |\mathbf{h}_{\ell}| \leq [\mathbf{s}_{\mathbf{x}_k}]_{\ell}, \\ 0, & \text{else.} \end{cases} \quad (60)$$

The width of the support is

$$\mathbf{s}_{\mathbf{x}_k} \triangleq \begin{cases} \mathbf{s}_k - \mathbf{r}_k, & \mathbf{r}_k, \mathbf{s}_k \in \mathbb{R}^N, \\ \mathbf{s}_k - \mathbf{r}_k + \mathbf{1}, & \mathbf{r}_k, \mathbf{s}_k \in \mathbb{Z}^N. \end{cases} \quad (61)$$

Note that discretized uniform random vectors have $\mathbf{x}_k / \Delta_{\mathbf{x}}, \mathbf{h} / \Delta_{\mathbf{x}}, \mathbf{r}_k / \Delta_{\mathbf{x}}, \mathbf{s}_k / \Delta_{\mathbf{x}} \in \mathbb{Z}^N$ whereas discrete uniform random vectors have $\mathbf{x}_k, \mathbf{h}, \mathbf{r}_k, \mathbf{s}_k \in \mathbb{Z}^N$ by definition. Thus, for the i.i.d. continuous uniform distribution and discretized distributions ($\mathbf{x}_k \in \mathbb{R}^N$)

$$\begin{aligned} \mathbf{r}_k &= \mathbf{m}_{\mathbf{x}_k} - 1/2\sqrt{12\text{diag}(\mathbf{C}_{\mathbf{x}_k})}, \\ \mathbf{s}_k &= \mathbf{m}_{\mathbf{x}_k} + 1/2\sqrt{12\text{diag}(\mathbf{C}_{\mathbf{x}_k})} \end{aligned} \quad (62)$$

whereas for the i.i.d. discrete uniform distribution ($\mathbf{x}_k \in \mathbb{Z}^N$)

$$\begin{aligned} \mathbf{r}_k &= \mathbf{m}_{\mathbf{x}_k} - 1/2\mathbf{1} - 1/2\sqrt{\mathbf{1} + 12\text{diag}(\mathbf{C}_{\mathbf{x}_k})}, \\ \mathbf{s}_k &= \mathbf{m}_{\mathbf{x}_k} - 1/2\mathbf{1} + 1/2\sqrt{\mathbf{1} + 12\text{diag}(\mathbf{C}_{\mathbf{x}_k})}. \end{aligned} \quad (63)$$

Vector $\mathbf{m}_{\mathbf{x}_k}$ denotes the mean of \mathbf{x}_k and $\mathbf{1}$ the one-vector. This leads to

$$\mathbf{s}_{\mathbf{x}_k} = \begin{cases} \sqrt{12\text{diag}(\mathbf{C}_{\mathbf{x}_k})}, & \mathbf{x}_k \in \mathbb{R}^N, \\ \sqrt{\mathbf{1} + 12\text{diag}(\mathbf{C}_{\mathbf{x}_k})}, & \mathbf{x}_k \in \mathbb{Z}^N. \end{cases} \quad (64)$$

Theorem 8 (SWW Bound/Uniform Distributions): Consider a linear continuous, discrete, or hybrid state-space model. Let the innovation noise, the measurement noise and the prior be uniform and independent. Furthermore, let the elements of the vectors be statistically independent. Then the SWW bound (25) is given by (43), (51), and (50) at the bottom of a previous page where all $\rho := \rho^U$.

Proof: The derivation proceeds as in the proof of Theorem 6 but uses Lemmas 18, 17, and 19 from the appendices. \blacksquare

Corollary 9 (Uniform Prior, Gaussian Noise): Consider a linear continuous, discrete, or hybrid state-transition equation. Let $v(\mathbf{x}_0 | \mathbf{x}_{-1}) := v(\mathbf{x}_0)$ be uniform, and both the measurement and the innovation noise be Gaussian. Then

$$\rho_{\mathbf{x}_0} := \rho_{\mathbf{x}_0}^U, \quad \rho_{\mathbf{w}_0} := \rho_{\mathbf{w}_0}^G \quad (65)$$

in (51).

Proof: The derivation proceeds as in the proof of Theorem 6 but uses Lemma 18. \blacksquare

The *finite support* of the uniform distribution induces bounds on the test-point matrix \mathbf{H}_k :

Proposition 10 (Box Conditions): Given a linear state-space model with multivariate independent uniform noise and prior. Then for all $k \geq 0$

$$-\mathbf{s}_{\mathbf{w}_k} \preceq \mathbf{h}_{k,a} \pm \mathbf{h}_{k,b} \preceq \mathbf{s}_{\mathbf{w}_k}, \quad (66a)$$

$$-\mathbf{s}_{\mathbf{w}_k} \preceq \Phi \mathbf{h}_{k,a} \pm \Phi \mathbf{h}_{k,b} \preceq \mathbf{s}_{\mathbf{w}_k}, \quad (66b)$$

$$-\mathbf{s}_{\mathbf{w}_k} \preceq \Phi \mathbf{h}_{k,a} \pm \mathbf{h}_{k,b} \preceq \mathbf{s}_{\mathbf{w}_k}, \quad (66c)$$

$$-\mathbf{s}_{\mathbf{v}_k} \preceq \mathbf{C}\mathbf{h}_{k,a} \pm \mathbf{C}\mathbf{h}_{k,b} \preceq \mathbf{s}_{\mathbf{v}_k}. \quad (66d)$$

Furthermore,

$$\mathbf{h}_{k,a} \neq \mathbf{0}, \quad \mathbf{h}_{k,b} \neq \mathbf{0}. \quad (66e)$$

Proof: Bounds (66a) to (66c) stem from (95) in Lemma 17. Bound (66d) stem in a similar way from (100) in Lemma 19.

If both $\mathbf{h}_{k,a} \rightarrow \mathbf{0}$ and $\mathbf{h}_{k,b} \rightarrow \mathbf{0}$, the SWW bound collapses to the SCR bound [13], [24]. For uniform distributions, the SCR bound does not exist because of the finite support and this leads to (66e). \blacksquare

The upper bounds are important constraints on \mathfrak{H}_k . Assume that $v(\mathbf{w}_k), k \in \mathbb{N}_0$, has a much larger support than the support of all other $v(\mathbf{w}_{k'}), k' \in \mathbb{N}_0 \setminus \{k\}$. Then the maximum possible $\mathbf{H}_{k'}$ is defined by the minimum \mathbf{H}_k through (65).

Proposition 11 (Equality of Bounds): Given the continuous model (34), the discrete model (45), and the hybrid model (45).

Let the PDs be independently uniformly distributed. Both, the discrete and the hybrid model are discretized continuous models and thus $\mathbf{x}_k/\Delta_{\mathbf{x}}, \mathbf{r}_k/\Delta_{\mathbf{x}}, \mathbf{s}_k/\Delta_{\mathbf{x}} \in \mathbb{Z}^N$. If

$$\mathfrak{J}_k/\Delta_{\mathbf{x}} \in \mathbb{Z}^{KN \times KN} \quad (67)$$

then the SWW bound of the discrete, the continuous, and the hybrid models are equal.

Proof: The proof proceeds as that of Proposition 7 but uses Lemmas 17 to 19 instead of Lemmas 14 to 16. ■

VI. ANALYTIC SOLUTION FOR EXPONENTIAL DISTRIBUTIONS

This section is devoted to the analytic SWW bound for models with either continuous or discretized multivariate independent exponential densities $\text{Exp}\{\boldsymbol{\alpha}_k\}$ [34], i.e.,

$$v(\mathbf{x}_k) \triangleq \prod_{\ell=1}^N \begin{cases} c'_\ell e^{-\alpha_\ell [\mathbf{x}_k]_\ell}, & [\mathbf{x}_k]_\ell \geq 0, \\ 0, & \text{else.} \end{cases} \quad (68)$$

Factor c'_ℓ normalizes the densities and parameter $\alpha_\ell \triangleq [\boldsymbol{\alpha}]_\ell \geq 0$. If \mathbf{x}_k is continuous, then $c'_\ell = \alpha_\ell$. Note that α_ℓ is the inverse of the mean and standard deviation of $[\mathbf{x}_k]_\ell$. It is convenient to define

$$\rho_{\mathbf{x}_k}^{\text{E}}(\mathbf{h}) \triangleq \prod_{\ell=1}^N \begin{cases} e^{\alpha_\ell/2h_\ell}, & h_\ell < 0, \\ e^{-\alpha_\ell/2h_\ell}, & \text{cont.}, h_\ell \geq 0, \\ e^{-\alpha_\ell/2h_\ell} c'_\ell \frac{e^{\alpha_\ell \Delta_{\mathbf{x}}}}{e^{\alpha_\ell \Delta_{\mathbf{x}} - 1}}, & \text{disc.}, h_\ell \geq 0, \\ \alpha_\ell \Delta_{\mathbf{x}} > 0 \end{cases} \quad (69)$$

with $h_\ell = [\mathbf{h}]_\ell$, $\alpha_\ell > 0$, and $h_\ell = \Delta_{\mathbf{x}} h_\ell^{\text{d}}$ for discretized densities.

Theorem 12 (SWW Bound/Exponential Distributions): Consider a linear continuous, discrete, or hybrid state-transition equation. Let the noise and the prior be defined by a multivariate independent exponential distribution.

Then the SWW bound (25) and (43) for the state vector \mathbf{x}_k is given by (50) at the bottom of a previous page where

$$\rho := \rho^{\text{E}}. \quad (70)$$

Proof: The derivation of the WW lower bound for Gaussian noise and prior (Theorem 6) leads to the proof. Starting with (29c), the BD (29h) is computed for the noise under consideration. A re-cast of the latter one is derived in (33). Next we use Corollary 5 and get multiplications of expectations. They compute as in Lemmas 20 and 21. Finally, we get (50) at the bottom of a previous page whereby $\rho_{\mathbf{x}} = \rho_{\mathbf{x}}^{\text{E}}$. ■

Corollary 13 (Prior): Consider a linear continuous, discrete, or hybrid state-transition equation. Let $v(\mathbf{y}_0|\mathbf{x}_0) := v_{\mathbf{y}_0}(\mathbf{y}_0)$ and $v(\mathbf{x}_0|\mathbf{x}_{-1}) := v(\mathbf{x}_0)$ be independently exponentially distributed. Then the SWW bound is given by Theorem 12 except that we utilize \mathbf{D}_1^{11} in (51) with

$$\rho_{\mathbf{x}_0}(\mathbf{h}) := \rho_{\mathbf{x}_0}^{\text{E}}(\mathbf{h}). \quad (71)$$

Proposition 7 for Gaussian distributions is not applicable for exponential distributions due to the additional factor $c'_\ell \frac{e^{\alpha_\ell \Delta_{\mathbf{x}}(1-h_\ell^{\text{d}})}}{e^{\alpha_\ell \Delta_{\mathbf{x}} - 1}}$ and the case differentiation in (69).

VII. PRACTICAL ISSUES

In the sequel, we address practical problems arising. Note that the test-point matrix \mathbf{H}_k defines a specific SWW bound of the SWW family.

A. Computational Effort

The non-sequential WW bound (23) computes $KN \times KN$ elements of \mathfrak{J}_k , where $K \in \mathbb{N}$ is the discrete time duration. This bound is quadratic in time whereas the SWW bound is constant, linear, or quadratic:

Consider the sequential WW bound (25) for a linear state-space model with an analytic solution (50). With (43), it requires the computation of $N \times N$ elements in each of the $3K$ matrices \mathbf{D}_{k+1}^{11} , \mathbf{D}_{k+1}^{12} , and \mathbf{D}_{k+1}^{22} . The number of operations to compute each element is independent of K . Hence, $3KN^2$ elements are computed and the effort is linear in time.

Moreover, if $v(\mathbf{y}_k|\mathbf{x}_k)$, $v(\mathbf{x}_{k+1}|\mathbf{x}_k)$, and the test-point matrix \mathbf{H}_k is constant for $k > 1$, then $\mathbf{D}_{k+1}^{ij} = \mathbf{D}_k^{ij}$, $i, j \in \{1, 2\}$. The computational effort is constant over time. Consider the general SWW bound (25) with (29), without closed-form solution ρ , and a state-space model with discrete multivariate distributions of finite support $[r_1, s_1]$. The expectation (29h) then simplifies to $K+1$ sums each $N_\zeta = N(s-r+1)$ summands. At each $k = 1, \dots, K$, (29h) is computed for 4 matrices \mathbf{D}_{k+1}^{01} , \mathbf{D}_{k+1}^{11} , \mathbf{D}_{k+1}^{12} , and \mathbf{D}_{k+1}^{22} of size $N \times N$. Thus, we obtain $4KN^2 \times (K+1)N_\zeta$, i.e., the effort is quadratic in time (cf. [35]).

B. Impact of the Test-Point Matrix

The optimal choice of the test-point matrix \mathfrak{J}_k maximizes the WW bound. Even without a general optimal solution to this maximization, we provide some useful guidelines. To keep the discussion simple, an one-dimensional linear transition model is considered with Gaussian, uniform, and exponential distributions, i.e.,

$$x_{k+1} = x_k + w_k, \quad (72a)$$

$$y_k = x_k + v_k, \quad (72b)$$

with $\sigma_{x_0}^2 = 0.4$, $\sigma_{w_k}^2 = 0.4$, $\sigma_{v_k}^2 = 0.4$. For Gaussian and uniform distributions $\mu_{x_0} = \mu_{w_k} = 0$ whereas for the exponential distributions $\mu_{x_0} = 1/\sigma_{x_0}$, $\mu_{w_k} = 1/\sigma_{w_k}$, and $\mu_{v_k} = 1/\sigma_{v_k}$. Fig. 1 plots the SWW bounds and sequential CR (SCR) bounds vs. $h_{1,k}$ at two time steps $k = 1$ and $k = 19$ [10].

The SCR bounds only exists for the twice differentiable Gaussian density. In that case, when $h_{1,k} \rightarrow 0$, the SWW bound approaches the SCR bound which is the optimum. For uniform distributions, the test points $h_{1,k}$ are box constrained by (66). Fig. 1 shows only the positive part of this allowed interval $(0, s]$ and the point of maximum SWW bound is close to $(s-r)/4$. Notice that at $k = 19$, where the influence of the prior is small, that the uniform prior / Gaussian noise case approaches the all-Gaussian case, i.e., the influence of the prior fades with time. The markers (◆) in Fig. 1 show the optimal test points $h_{1,k}$ obtained numerically. Observe that the high mode of the exponential density at $w_k = v_k = x_0 = 0_+$ lowers its bound.

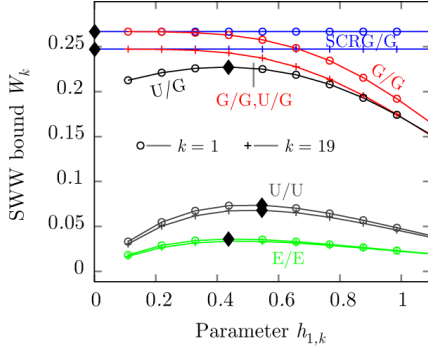


Fig. 1. Impact of $h_{1,k}$ on the SWW bound for the state x_k (71a) for Gaussian prior/noise (G/G), uniform prior/Gaussian noise (U/G), uniform prior/noise (U/U), and exponential prior/noise (E/E). For small $h_{1,k}$, the G/G SWW bounds approach the SCR bounds. Markers (\blacklozenge) indicate the optimal $h_{1,k}$ for maximum SWW.

For dimensions greater than one, it is more difficult to obtain optimal matrices $\mathbf{H}_k, k \in \mathbb{N}_+$. The ℓ th row of the transition matrix Φ specifies its dependency on all states. Similarly, the ℓ th column of the \mathbf{H}_k specifies, which states are considered for the computation of the ℓ th-state's SWW bound. This suggests that the positions of non-zero elements in \mathbf{H}_k should agree with Φ^T .

The tightness of the SWW bound depends on two contrary effects of \mathbf{H}_k . For illustration, consider a one-dimensional state-space models with test point $h_k < 1$. On one hand (Effect 1), small h_k gives Bayesian Bhattacharyya coefficient ≈ 1 and hence D_k in (50) becomes small. The difference (43) becomes small, which in turn leads to high J_k^{-1} . On the other hand (Effect 2), $h_k^2 J_k^{-1}$ in (25) is a quadratic form where h_k^2 occurs, i.e., it lowers the bound.

For Gaussian distributions, if $h_k \downarrow 0$, the coefficients go faster to 1 than $h_k^2 J_k^{-1} \downarrow 0$. This is seen by inserting approximation (54) and (43) into (25) with $h_k = h \rightarrow 0$, $\sigma_{w_k} = \sigma_w$, and $\sigma_{v_k} = \sigma_v$ i.e.,

$$W_{k+1} = \frac{h^2}{J_{k+1}} \approx \frac{1}{\frac{1}{\sigma_w^2} - \frac{C^2}{\sigma_v^2} + \underbrace{\frac{\Phi}{\sigma_w^4 (J_k/h^2 + \Phi^2/\sigma_w^2)}}_{w_k}} \quad (73)$$

(cf. (4.43) to (4.45) in [10]). Here, the h^2 cancels, which is not true for non-Gaussian distributions whose coefficients are not approximately linear functions of h^2 for $h \rightarrow 0$. Eventually, Effect 1 is stronger than Effect 2 and hence the bound is tight.

At $h = 0+$, the derivatives of the Bayesian Bhattacharyya coefficient for i.i.d exponential, uniform, and Gaussian distributions are ordered,

$$\begin{aligned} \partial_h \rho^E|_{h=0+} &= -\frac{\alpha^2}{\sqrt{4}} = -\frac{1}{\sqrt{4\sigma^2}} \\ < \partial_h \rho^U|_{h=0+} &= -\frac{1}{\sqrt{12\sigma^2}} \\ < \partial_h \rho^G|_{h=0} &= -\frac{1}{4\sigma^2} h e^{-\frac{h_k^2}{8\sigma_k^2}} \Big|_{h=0} = 0. \end{aligned} \quad (74)$$

The smaller the derivatives, the more dominant Effect 2 and the looser the bound (cf. Fig. 1). Thus the SWW bound for exponential distributions is the loosest (cf. example in Section VIII).

C. Computation of the Prior

Consider a hybrid model (45) where the state \mathbf{x}_0^c is modeled by

$$\mathbf{x}_0^c = \sum_{\ell=-K}^{-1} (\Phi^c)^{1-\ell} \Phi^{cd}(\mathbf{x}_\ell^d) + \mathbf{w}_\ell \quad (75)$$

with time horizon K . Function Φ^{cd} might be a source in an acoustic field with the sum representing the evolution of the corresponding acoustic field during K time steps [5]. The prior $v(\mathbf{x}_0^c, \mathbf{x}_0^d)$ is computed by marginalizing the joint probability density

$$v(\mathbf{x}_{-K:0}) = v(\mathbf{x}_{-K}) \prod_{\ell=-K}^{-1} v(\mathbf{x}_{\ell+1}|\mathbf{x}_\ell). \quad (76)$$

Fortunately, the explicit computation of the marginal $v(\mathbf{x}_0)$ is not necessary in our context since we are only interested in the lower bound of the mean-square error and not in the PD itself. Therefore we assume a known PD at time $-K$, i.e., it carries over the role of the prior. The SWW bound (25) recursively computes the WW bound until time 0. Clearly, in this time interval no measurements influence the bound, i.e.,

$$v(\mathbf{y}_\ell|\mathbf{x}_\ell) = v(\mathbf{y}_\ell), \quad \forall \ell \leq 0. \quad (77)$$

Due to the existence of a density and the independence of the states, the expectations (38b) reduces to $\int v(\mathbf{y}_\ell) d\lambda_{\mathbf{y}_\ell} = 1$ for $\ell = -K, \dots, 0$. This causes $\rho_{v_\ell} = 1$ in (50). Briefly speaking, our approach uses a simplified version of the SWW recursion instead of the explicit computation of the prior at time zero.

D. Partly-Deterministic Transition Equations

An interesting problem occurs when some parts of the transition equation (for instance (21a)) are deterministic, i.e., no noise is added. This results in a singular matrix $\mathbb{E}\{\mathbf{x}_k \mathbf{x}_k^T\}$. This causes the Bayesian bounds to become singular (cf. Section II-B). For SCR bounds, [18] performs regularization by assuming additive noise with small variance. This may meet most physical problems, so does a discretized physical field.

VIII. EXAMPLES

In this section, the following linear state-space model demonstrates the bounds derived for different distributions:

$$\mathbf{x}_{k+1} = \begin{bmatrix} 1 & 1 & 0 \\ 0 & 1 & 0 \\ 0 & 0 & 1 \end{bmatrix} \mathbf{x}_k + \mathbf{w}_k, \quad (78a)$$

$$\mathbf{y}_k = \begin{bmatrix} 1 & 0 & 0 \\ 0 & 0 & 1 \end{bmatrix} \mathbf{x}_k + \mathbf{v}_k. \quad (78b)$$

The first state $[\mathbf{x}_k]_1$ depends on itself and the second $[\mathbf{x}_k]_2$ whereas the others depend only on themselves. Equation (78b) measures $[\mathbf{x}_k]_1$ and $[\mathbf{x}_k]_3$.

We plot the diagonals of the SWW bound \mathbf{W}_k (25) with the arbitrary test-point matrix

$$\mathbf{H}_k = [\mathbf{h}_{k,1} \quad \mathbf{h}_{k,2} \quad \mathbf{h}_{k,3}] := \begin{bmatrix} h_{\text{opt}} & 0 & 0 \\ h_{\text{opt}}/2 & h_{\text{opt}} & 0 \\ 0 & 0 & h_{\text{opt}} \end{bmatrix}. \quad (79)$$

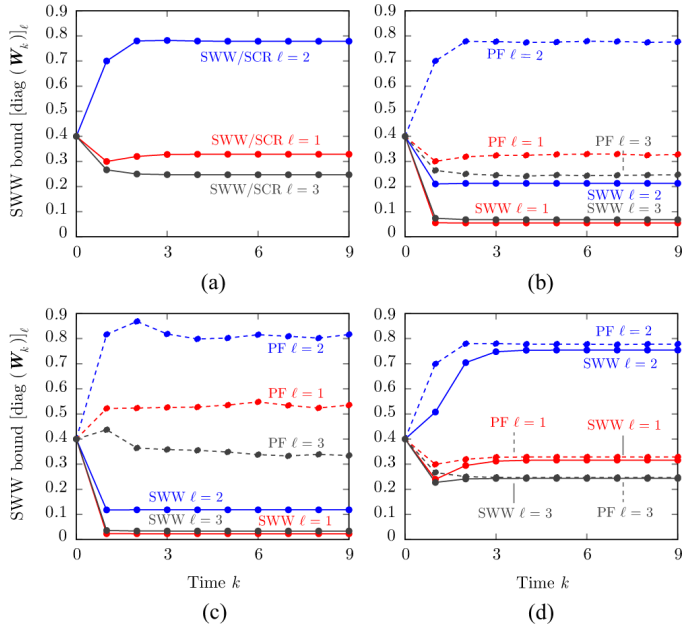


Fig. 2. The SWW lower bounds for the ℓ th element of \mathbf{x}_k [cf. (78)] for (a) continuous/discretized Gaussian prior/noise, (b) continuous/discretized uniform prior/noise, (c) continuous exponential prior/noise, and (d) continuous uniform prior/Gaussian noise. Additionally, in (a) the SCR bound and in (b)–(d) the mean-square error of a particle filter are shown. Time $k = 0$ shows the prior error variance.

The computation of Element $[\mathbf{W}_k]_{ab}$ utilizes vectors $\mathbf{h}_{k,a}$ and $\mathbf{h}_{k,b}$ for $a, b \in \{1, 2, 3\}$. Although Fig. 2 shows only the diagonals of \mathbf{W}_k , i.e., the bound on the mean-square error, update (43) demands for the non-diagonal elements of \mathbf{W}_k .

We discuss four settings for continuous distributions in Fig. 2: the all-Gaussian, the uniform prior/Gaussian noise, the all-uniform, and the all-exponential case. Their covariance matrices are $\mathbf{C}_{\mathbf{x}_0} = \mathbf{C}_{\mathbf{w}_k} = 0.4\mathbf{I}$ and $\mathbf{C}_{\mathbf{v}_k} = 0.4\mathbf{I}$. The Gaussian and uniform distributions have zero-mean. The means of the exponential distributions equal their standard deviations.

The all-Gaussian case is plotted in Fig. 2(a). The SCR bound exists and is shown as [10]. The test point $h_{\text{opt}} = 0.01095$ and the SWW bound approaches the SCR bound. The SCR bound is achieved using a Kalman filter. State $\ell = 3$ is observed and has the lowest bound. State $\ell = 1$ depends additionally on state $\ell = 2$ and hence has a higher bound. State $\ell = 2$ is not directly observed and thus has the highest bound.

The all-uniform case, Fig. 2(b) is similar to the all-Gaussian case except that the SWW bounds of the observed states are close together. The test point $h_{\text{opt}} = 0.514$ is the value of the tightest SWW bound. The all-exponential case is demonstrated in Fig. 2(c) with $h_{\text{opt}} = 0.47$. Fig. 2(d) shows the SWW bound for uniform prior and Gaussian noise with $h_{\text{opt}} = 0.427$. Compared with the all-Gaussian case we only see a difference at time $k = 1$ (initial phase).

For the non-Gaussian densities, Figs. 2(b)–2(d) show the mean-square error of an importance-sampling-resampling particle filter using the transition density as importance function, 20000 particles, and 1000 realizations [10], [36]. The order of the SWW's tightness corresponds to the derivative of the Bayesian Bhattacharyya coefficient (74) at the origin.

We use model (78) and test-point matrix (79) again for discretized Gaussian and discretized uniform densities. We seek for settings leading to the same SWW bounds for discretized and continuous distributions.

Since Gaussian densities have infinite support, using their discretized versions with quantization step size $\Delta_x = 0.00219$ and $h_{\text{opt}}^d = 5$ give the same SWWs as the continuous cases (see Fig. 2).

The width (64) of the continuous uniform density computes to $\varsigma_{\mathbf{x}_k} = 2.19 \times 1$. Let the discrete uniform density have a width of the support $\varsigma_{\mathbf{x}_k}^d = 20 \times 1$. Then with (67), the quantization step size is $\Delta_x = 0.1152$ and the covariance matrix of the discrete uniform distributions are $\mathbf{C}_{\mathbf{x}_0} = \mathbf{C}_{\mathbf{w}_k} = 1/12(\varsigma_{\mathbf{x}_k}^{d,2} - 1)\mathbf{I}$ and $\mathbf{C}_{\mathbf{v}_k} = 1/12(\varsigma_{\mathbf{x}_k}^{d,2} - 1)\mathbf{I}$. Now the SWW bound for the discrete (quantized) uniform distribution $\text{Unif}\{-\varsigma_{\mathbf{x}_k}^d/2, \varsigma_{\mathbf{x}_k}^d/2\}$ equals that of the continuous case.

The next example demonstrates a hybrid model with discrete $[\mathbf{x}_k]_2$. Therefore, (78a) becomes

$$\begin{bmatrix} x_{1,k+1}^c \\ x_{2,k+1}^d \\ x_{3,k+1}^c \end{bmatrix} = \begin{bmatrix} 1 & 1 & 0 \\ 0 & 1 & 0 \\ 0 & 0 & 1 \end{bmatrix} \begin{bmatrix} x_{1,k}^c \\ x_{2,k}^d \\ x_{3,k}^c \end{bmatrix} + \begin{bmatrix} w_{1,k}^c \\ w_{2,k}^d \\ w_{3,k}^c \end{bmatrix}, \quad (80a)$$

with

$$w_{2,k}^d \sim \frac{1}{c''} f_{w_{2,k}^c}(w_{2,k}^d), \quad x_{2,0}^d \sim \frac{1}{c'''} f_{x_{2,0}^c}(x_{2,0}^d). \quad (80b)$$

Constants c'' and c''' are normalizing factors. Equation (80a) and (80b) form a hybrid model similar to (45). The quantization interval equals the test point $h_{\text{opt}} = \Delta_x = 0.01905$, and the continuous distributions are Gaussian as the first example. The bound for $x_{2,k}^d$ equals the bound for $x_{2,k}$ in (78a) and is shown in Fig. 2(a) (cf. Proposition 7).

We discuss and analyze a different example of a hybrid model with Gaussian and discretized uniform distributions in [35].

IX. CONCLUSION

The family of Weiss–Weinstein bounds enables the use of hybrid discrete and continuous state-vectors. The use of the Bayesian Bhattacharyya coefficient gives a general recursion for the sequential bound. We provide analytic solutions for Gaussian, uniform, and exponential distributions and their discrete approximations stemming from discretized states.

The SWW bound depends on the test-point matrix \mathfrak{H}_k . An optimal \mathfrak{H}_k gives the tightest bound. The finite support of uniform densities causes box constraints on \mathfrak{H}_k . For Gaussian distribution, the optimal $\mathfrak{H}_k \rightarrow \mathbf{0}$ in which it can in certain cases give the sequential Cramér–Rao bound.

The optimal \mathfrak{H}_k for uniform distributions lies near the middle of the box constraint's interval. The tightness of the bound depends on the derivative of the Bayesian Bhattacharyya distribution in the origin.

The shape of the transition matrix describes the dependency between states. Thus, it influences the optimum choice of \mathfrak{H}_k that describes the influence of noise on these states. The SWW bounds for continuous and discretized states are equal for specific choices of the bound's test-point matrix \mathfrak{H}_k . The derivations concerning discretized states are applicable for discretized measurements as well.

Further results are related to practical issues. For linear state-space models with analytic solutions the computational effort increases linear with time. Additionally, if the noise statistics are time-invariant, then the effort is constant. If the prior density stems from a recursion, it is possible to compute the SWW bound without explicit prior.

APPENDIX A GAUSSIAN DENSITIES

The following Lemmas are independent of the discrete or continuous nature of the densities. The densities are either Gaussian densities or discretized Gaussian densities $p(\mathbf{w}_k^d) = \frac{1}{c''} f_{\mathbf{w}_k}(\mathbf{w}_k^d)$ or $p(\mathbf{v}_k^d) = \frac{1}{c''} f_{\mathbf{v}_k}(\mathbf{v}_k^d)$. The factor c'' normalizes the PMF.

We use the weighted inner-product $\langle \mathbf{x}_1, \mathbf{x}_2 \rangle_{\mathbf{C}_x^{-1}} \triangleq \mathbf{x}_1^T \mathbf{C}_x^{-1} \mathbf{x}_2$.

Lemma 14 (Gaussian Innovation Noise): For a Gaussian innovation noise, the solution of (38a) is

$$E_{k+1} = \rho_{\mathbf{w}_k}^G (\mathbf{h}_{k+1,a} - \Phi \mathbf{h}_{k,a} + \mathbf{h}_{k+1,b} - \Phi \mathbf{h}_{k,b}) \quad (81)$$

which is independent of \mathbf{x}_k (cf. Lemma 3).

Proof: Let us insert the Gaussian density into (38a), i.e.,

$$E_{\mathbf{x}_{k+1} | \mathbf{x}_k} \left\{ \frac{e^{-\frac{1}{4} \|\mathbf{x}_{k+1} + \mathbf{h}_{k+1,a} - \Phi(\mathbf{x}_k + \mathbf{h}_{k,a})\|^2} c_{\mathbf{w}_k}^{-1}}}{e^{-\frac{1}{2} \|\mathbf{x}_{k+1} - \Phi \mathbf{x}_k\|^2} c_{\mathbf{w}_k}^{-1}} \times e^{-\frac{1}{4} \|\mathbf{x}_{k+1} - \mathbf{h}_{k+1,b} - \Phi(\mathbf{x}_k - \mathbf{h}_{k,b})\|^2} c_{\mathbf{w}_k}^{-1}} \right\}. \quad (82)$$

This simplifies to

$$c'_{\mathbf{w}} \int_{-\infty}^{\infty} e^{-1/2 \|\mathbf{x}_{k+1} - \Phi \mathbf{x}_k\|_{\mathbf{C}_{\mathbf{w}_k}}^2} \times e^{-1/4 \|\mathbf{h}_{k+1,a} - \Phi \mathbf{h}_{k,a}\|_{\mathbf{C}_{\mathbf{w}_k}^{-1}} - 1/4 \|\mathbf{h}_{k+1,b} + \Phi \mathbf{h}_{k,b}\|_{\mathbf{C}_{\mathbf{w}_k}^{-1}}} \times e^{-1/2 \langle \mathbf{x}_{k+1} - \Phi \mathbf{x}_k, \mathbf{h}_{k+1,a} - \Phi \mathbf{h}_{k,a} - \mathbf{h}_{k+1,b} + \Phi \mathbf{h}_{k,b} \rangle_{\mathbf{C}_{\mathbf{w}_k}^{-1}}} d\lambda_{\mathbf{x}_{k+1}} \quad (83)$$

where

$$c'_{\mathbf{w}} \triangleq \begin{cases} (2\pi)^{-N/2} \det(\mathbf{C}_{\mathbf{w}_k})^{-1/2}, & \text{continuous,} \\ (2\pi)^{-N/2} \det(\mathbf{C}_{\mathbf{w}_k})^{-1/2} c'', & \text{discretized.} \end{cases} \quad (84)$$

We substitute

$$\|\mathbf{t}\|_{\mathbf{C}_{\mathbf{w}_k}^{-1}}^2 := \|\mathbf{x}_{k+1} - \Phi \mathbf{x}_k\|_{\mathbf{C}_{\mathbf{w}_k}^{-1}}^2 + \langle \mathbf{x}_{k+1} - \Phi \mathbf{x}_k, \mathbf{h}_{k+1,a} - \Phi \mathbf{h}_{k,a} - \mathbf{h}_{k+1,b} + \Phi \mathbf{h}_{k,b} \rangle_{\mathbf{C}_{\mathbf{w}_k}^{-1}} + \frac{1}{4} \|\mathbf{h}_{k+1,a} - \Phi \mathbf{h}_{k,a} - \mathbf{h}_{k+1,b} + \Phi \mathbf{h}_{k,b}\|_{\mathbf{C}_{\mathbf{w}_k}^{-1}}^2$$

and utilize

$$c'_{\mathbf{w}} \int_{-\infty}^{\infty} e^{-1/2 \|\mathbf{t}\|_{\mathbf{C}_{\mathbf{w}_k}^{-1}}^2} d\lambda_{\mathbf{t}} = 1 \quad (85)$$

to obtain the final result. \blacksquare

Lemma 15 (Gaussian Prior): For a Gaussian prior, the solution of (38a) is

$$E_1 = \rho_{\mathbf{x}_0}^G (\mathbf{h}_{0,a} + \mathbf{h}_{0,b}). \quad (86)$$

Proof: The results follows from Lemma 14 where $v(\mathbf{x}_0 | \mathbf{x}_{-1}) = v_{\mathbf{x}_0}(\mathbf{x}_0)$ and $\mathbf{h}_{-1,a} + \mathbf{h}_{-1,b} = 0$. \blacksquare

Lemma 16 (Gaussian Measurement Noise): For a Gaussian measurement noise the solution of (38b) is

$$E'_{k+1} = \rho_{\mathbf{v}_{k+1}}^G (\mathbf{C} \mathbf{h}_{k+1,a} + \mathbf{C} \mathbf{h}_{k+1,b}) \quad (87)$$

which is independently of \mathbf{x}_{k+1} (cf. Corollary 4).

Proof: Let us insert the Gaussian density into (38b), i.e.,

$$E_{\mathbf{y}_{k+1} | \mathbf{x}_{k+1}} \left\{ \frac{e^{-\frac{1}{4} \|\mathbf{y}_{k+1} - \mathbf{C}(\mathbf{x}_{k+1} + \mathbf{h}_{k+1,a})\|^2} c_{\mathbf{v}_{k+1}}^{-1}}}{e^{-\frac{1}{2} \|\mathbf{y}_{k+1} - \mathbf{C} \mathbf{x}_{k+1}\|_{\mathbf{C}_{\mathbf{v}_{k+1}}^{-1}}} \times e^{-\frac{1}{4} \|\mathbf{y}_{k+1} - \mathbf{C}(\mathbf{x}_{k+1} - \mathbf{h}_{k+1,b})\|^2} c_{\mathbf{v}_{k+1}}^{-1}} \right\}. \quad (88)$$

This simplifies to

$$c'_{\mathbf{v}} \int_{-\infty}^{\infty} e^{-1/2 \|\mathbf{y}_{k+1} - \mathbf{C} \mathbf{x}_{k+1}\|_{\mathbf{C}_{\mathbf{v}_{k+1}}^{-1}} - 1/4 \|\mathbf{C} \mathbf{h}_{k,a}\|_{\mathbf{C}_{\mathbf{v}_{k+1}}^{-1}} - 1/4 \|\mathbf{C} \mathbf{h}_{k,b}\|_{\mathbf{C}_{\mathbf{v}_{k+1}}^{-1}}} \times e^{-1/2 \langle \mathbf{y}_{k+1} - \mathbf{C} \mathbf{x}_{k+1}, \mathbf{C} \mathbf{h}_{k,a} - \mathbf{C} \mathbf{h}_{k,b} \rangle_{\mathbf{C}_{\mathbf{v}_{k+1}}^{-1}}} d\lambda_{\mathbf{y}_{k+1}} \quad (89)$$

where

$$c'_{\mathbf{v}} \triangleq \begin{cases} (2\pi)^{-N/2} \det(\mathbf{C}_{\mathbf{v}_{k+1}})^{-1/2}, & \text{continuous,} \\ (2\pi)^{-N/2} \det(\mathbf{C}_{\mathbf{v}_{k+1}})^{-1/2} c'', & \text{discretized.} \end{cases} \quad (90)$$

We substitute

$$\|\mathbf{t}\|_{\mathbf{C}_{\mathbf{v}_{k+1}}^{-1}}^2 := \|\mathbf{y}_{k+1} - \mathbf{C} \mathbf{x}_{k+1}\|_{\mathbf{C}_{\mathbf{v}_{k+1}}^{-1}}^2 - \langle \mathbf{y}_{k+1} - \mathbf{C} \mathbf{x}_{k+1}, \mathbf{C} \mathbf{h}_{k+1,a} - \mathbf{C} \mathbf{h}_{k+1,b} \rangle_{\mathbf{C}_{\mathbf{v}_{k+1}}^{-1}} + \frac{1}{4} \|\mathbf{C} \mathbf{h}_{k+1,a} - \mathbf{C} \mathbf{h}_{k+1,b}\|_{\mathbf{C}_{\mathbf{v}_{k+1}}^{-1}}^2$$

and utilize

$$c'_{\mathbf{v}} \int_{-\infty}^{\infty} e^{-1/2 \|\mathbf{t}\|_{\mathbf{C}_{\mathbf{v}_{k+1}}^{-1}}^2} d\lambda_{\mathbf{t}} = 1 \quad (91)$$

to obtain the final result. \blacksquare

APPENDIX B UNIFORM DENSITIES

The following Lemmas are independent of the discrete or continuous nature of the densities. The densities are either continuous or discrete uniform densities.

Lemma 17 (Uniform Innovation Noise): For an independent uniform density $v(\mathbf{w}_k)$, the solution of (38a) is

$$E_{k+1} = \rho_{\mathbf{w}_k}^U (\mathbf{h}_{k+1,a} - \Phi \mathbf{h}_{k,a} + \mathbf{h}_{k+1,b} - \Phi \mathbf{h}_{k,b}) \quad (92)$$

which is independent of \mathbf{x}_k .

Proof: Let us insert the uniform density into (38a), i.e.,

$$E_{\mathbf{x}_{k+1} | \mathbf{x}_k} \left\{ \frac{v_{\mathbf{w}_k}(\mathbf{x}_{k+1} + \mathbf{h}_{k+1,a} - \Phi(\mathbf{x}_k + \mathbf{h}_{k,a}))^{1/2}}{v_{\mathbf{w}_k}(\mathbf{x}_{k+1} - \Phi \mathbf{x}_k)} \times v_{\mathbf{w}_k}(\mathbf{x}_{k+1} - \mathbf{h}_{k+1,b} - \Phi(\mathbf{x}_k - \mathbf{h}_{k,b}))^{1/2} \right\}. \quad (93)$$

Due to the existence of a density, we have

$$\begin{aligned} & \int_{-\infty}^{\infty} v_{\mathbf{w}_k}(\mathbf{x}_{k+1} + \mathbf{h}_{k+1,a} - \Phi(\mathbf{x}_k + \mathbf{h}_{k,a}))^{1/2} \\ & \times v_{\mathbf{w}_k}(\mathbf{x}_{k+1} - \mathbf{h}_{k+1,b} - \Phi(\mathbf{x}_k - \mathbf{h}_{k,b}))^{1/2} d\lambda_{\mathbf{x}_{k+1}} \\ & = \int_{\mathbf{r}_k}^{\mathbf{s}_k} \prod_{\ell=1}^N \frac{\mathbb{1}_{\mathbf{x}_{k+1} + \mathbf{h}_{k+1,a} - \Phi(\mathbf{x}_k + \mathbf{h}_{k,a}) \in [\mathbf{r}_k, \mathbf{s}_k]}}{[\mathbf{s}_{\mathbf{w}_k}]_{\ell}} \\ & \times \mathbb{1}_{\mathbf{x}_{k+1} - \mathbf{h}_{k+1,b} - \Phi(\mathbf{x}_k - \mathbf{h}_{k,b}) \in [\mathbf{r}, \mathbf{s}]} d\lambda_{\mathbf{x}_k} \\ & = \prod_{\ell=1}^N \left[1 - \frac{|\mathbf{h}_{k+1,a} - \Phi \mathbf{h}_{k,a} + \mathbf{h}_{k+1,b} - \Phi \mathbf{h}_{k,b}|_{\ell}}{[\mathbf{s}_{\mathbf{w}_k}]_{\ell}} \right] \end{aligned} \quad (94)$$

if

$$|\mathbf{h}_{k+1,a} - \Phi \mathbf{h}_{k,a} + \mathbf{h}_{k+1,b} - \Phi \mathbf{h}_{k,b}|_{\ell} \leq [\mathbf{s}_{\mathbf{w}_k}]_{\ell} \quad (95)$$

else zero. ■

Lemma 18 (Uniform Prior): For an independent uniform density $v(\mathbf{w}_0)$, the solution of (38a) is

$$E_1 = \rho_{\mathbf{w}_k}^{\text{U}}(\mathbf{h}_{0,a} + \mathbf{h}_{0,b}). \quad (96)$$

Proof: The results follows from Lemma 17 where $v(\mathbf{x}_0 | \mathbf{x}_{-1}) = v_{\mathbf{x}_0}(\mathbf{x}_0)$ and $\mathbf{h}_{-1,a} + \mathbf{h}_{-1,b} = \mathbf{0}$. ■

Lemma 19 (Uniform Measurement Noise): For an independent uniform density $v(\mathbf{v}_k)$, the solution of (38b) is

$$E'_{k+1} = \rho_{\mathbf{v}_k}^{\text{U}}(-\mathbf{C}\mathbf{h}_{k+1,a} - \mathbf{C}\mathbf{h}_{k+1,b}) \quad (97)$$

which is independent of \mathbf{x}_{k+1} .

Proof: We insert the uniform density into (38b), i.e.,

$$\begin{aligned} E_{\mathbf{y}_{k+1} | \mathbf{x}_{k+1}} & \left\{ \frac{v_{\mathbf{v}_k}(\mathbf{y}_{k+1} - \mathbf{C}(\mathbf{x}_{k+1} + \mathbf{h}_{k+1,a}))^{1/2}}{v_{\mathbf{v}_k}(\mathbf{y}_{k+1} - \mathbf{C}\mathbf{x}_{k+1})} \right. \\ & \left. \times v_{\mathbf{v}_k}(\mathbf{y}_{k+1} - \mathbf{C}(\mathbf{x}_{k+1} - \mathbf{h}_{k+1,b}))^{1/2} \right\}. \end{aligned} \quad (98)$$

Due to the existence of a density, we have

$$\begin{aligned} & \int_{-\infty}^{\infty} v_{\mathbf{v}_{k+1}}(\mathbf{y}_{k+1} - \mathbf{C}(\mathbf{x}_{k+1} + \mathbf{h}_{k+1,a}))^{1/2} \\ & \times v_{\mathbf{v}_{k+1}}(\mathbf{y}_{k+1} - \mathbf{C}(\mathbf{x}_{k+1} - \mathbf{h}_{k+1,b}))^{1/2} d\lambda_{\mathbf{y}_{k+1}} \\ & = \int_{\mathbf{r}_{k+1}}^{\mathbf{s}_{k+1}} \prod_{\ell=1}^N \frac{\mathbb{1}_{\mathbf{y}_{k+1} - \mathbf{C}(\mathbf{x}_{k+1} + \mathbf{h}_{k+1,a}) \in [\mathbf{r}_{k+1}, \mathbf{s}_{k+1}]}}{[\mathbf{s}_{\mathbf{v}_k}]_{\ell}} \\ & \times \mathbb{1}_{\mathbf{y}_{k+1} - \mathbf{C}(\mathbf{x}_{k+1} - \mathbf{h}_{k+1,b}) \in [\mathbf{r}_{k+1}, \mathbf{s}_{k+1}]} d\lambda_{\mathbf{y}_{k+1}} \\ & = \prod_{\ell=1}^N \left[1 - \frac{|[\mathbf{C}\mathbf{h}_{k+1,a} + \mathbf{C}\mathbf{h}_{k+1,b}]_{\ell}|}{[\mathbf{s}_{\mathbf{v}_k}]_{\ell}} \right] \end{aligned} \quad (99)$$

if

$$|[\mathbf{C}\mathbf{h}_{k+1,a} + \mathbf{C}\mathbf{h}_{k+1,b}]_{\ell}| \leq [\mathbf{s}_{\mathbf{v}_k}]_{\ell} \quad (100)$$

else zero. ■

APPENDIX C EXPONENTIAL DENSITIES

We assume both exponential densities and discretized exponential densities $p(\mathbf{w}_k^{\text{d}}) = \frac{1}{c^{\text{T}} \mathbf{f}_{\mathbf{w}_k}(\mathbf{w}_k^{\text{d}})}$ and $p(\mathbf{v}_k^{\text{d}}) = \frac{1}{c^{\text{T}} \mathbf{f}_{\mathbf{v}_k}(\mathbf{v}_k^{\text{d}})}$. The factor $c'' = c_1'' \cdots c_N''$ normalizes the PMF.

Lemma 20 (Innovation Noise): Given a multivariate independent exponential density $v(\mathbf{w}_k)$, the solution of (38a) is

$$E_{k+1} = \rho_{\mathbf{w}_k}^{\text{E}}(\mathbf{h}_{k+1,a} - \Phi \mathbf{h}_{k,a} + \mathbf{h}_{k+1,b} - \Phi \mathbf{h}_{k,b}) \quad (101)$$

which is independent of \mathbf{x}_k .

Proof: Let us insert the density into (38a) and substitute $\mathbf{w} := \mathbf{x}_{k+1} - \mathbf{h}_{k+1,b} - \Phi(\mathbf{x}_k - \mathbf{h}_{k,b})$, $h_{\ell} = [\mathbf{h}_{k+1,a} - \Phi \mathbf{h}_{k,a} + \mathbf{h}_{k+1,b} - \Phi \mathbf{h}_{k,b}]_{\ell}$, and $w_{\ell} = [\mathbf{w}]_{\ell} + h_{\ell}$, i.e.,

$$\begin{aligned} & \int_{-\infty}^{\infty} v_{\mathbf{w}_k}(\mathbf{x}_{k+1} + \mathbf{h}_{k+1,a} - \Phi(\mathbf{x}_k + \mathbf{h}_{k,a}))^{1/2} \\ & \times v_{\mathbf{w}_k}(\mathbf{x}_{k+1} - \mathbf{h}_{k+1,b} - \Phi(\mathbf{x}_k - \mathbf{h}_{k,b}))^{1/2} d\lambda_{\mathbf{x}_{k+1}} \\ & = \prod_{\ell=1}^N \int_{-\infty}^{\infty} c'_{\ell} e^{-\alpha_{\ell}/2(w_{\ell} + h_{\ell}) - \alpha_{\ell}/2w_{\ell}} \\ & \times \mathbb{1}_{w_{\ell} + h_{\ell} \in [0, \infty)} \mathbb{1}_{w_{\ell} \in [0, \infty)} d\lambda_{w_{\ell}} \end{aligned} \quad (102)$$

where

$$c'_{\ell} = \begin{cases} \alpha_{\ell}, & v(w_{\ell}) \text{ cont.}, \\ \alpha_{\ell} c''_{\ell}, & v(w_{\ell}) \text{ discr.}, \end{cases} \quad (103)$$

normalizes the densities. We further get

$$\begin{aligned} & \prod_{\ell=1}^N c'_{\ell} e^{-\alpha_{\ell}/2h_{\ell}} \int_{h_{\ell}}^{\infty} e^{-\alpha_{\ell}(w_{\ell} - h_{\ell})} \mathbb{1}_{w_{\ell} \in [0, \infty)} d\lambda_{w_{\ell}} \\ & = \prod_{\ell=1}^N \begin{cases} e^{\alpha_{\ell}/2h_{\ell}}, & h_{\ell} < 0, \\ e^{\alpha_{\ell}/2h_{\ell}} c'_{\ell} \int_{h_{\ell}}^{\infty} e^{-\alpha_{\ell}w_{\ell}} d\lambda_{w_{\ell}}, & h_{\ell} \geq 0. \end{cases} \end{aligned} \quad (104)$$

For discrete w_{ℓ} , we define $h_{\ell} = \Delta_{\mathbf{x}} h_{\ell}^{\text{d}}$, $h_{\ell}^{\text{d}} \in \mathbb{Z}$. Thus,

$$\begin{aligned} \int_{h_{\ell}}^{\infty} e^{-\alpha_{\ell}w_{\ell}} d\lambda_{w_{\ell}} & = \sum_{w'_{\ell} = h_{\ell}^{\text{d}}}^{\infty} e^{-\alpha_{\ell} \Delta_{\mathbf{x}} w'_{\ell}} \\ & = \frac{e^{\alpha_{\ell} \Delta_{\mathbf{x}} (1 - h_{\ell}^{\text{d}})}}{e^{\alpha_{\ell} \Delta_{\mathbf{x}} - 1}} \text{ when } \alpha_{\ell} \Delta_{\mathbf{x}} > 0. \end{aligned} \quad (105)$$

The case $h_{\ell} \geq 0$ in (103) computes to

$$\begin{cases} e^{-\alpha_{\ell}/2h_{\ell}}, & v(w_{\ell}) \text{ cont.}, \\ e^{-\alpha_{\ell}/2\Delta_{\mathbf{x}} h_{\ell}^{\text{d}}} c'_{\ell} \frac{e^{\alpha_{\ell} \Delta_{\mathbf{x}}}}{e^{\alpha_{\ell} \Delta_{\mathbf{x}} - 1}}, & v(w_{\ell}) \text{ disc.}, \alpha_{\ell} \Delta_{\mathbf{x}} > 0, \end{cases} \quad (106)$$

neglecting $\alpha_{\ell} = 0$ for discretized densities. Eventually, this gives

$$\prod_{\ell=1}^N \begin{cases} e^{\alpha_{\ell}/2h_{\ell}}, & h_{\ell} < 0, \\ e^{-\alpha_{\ell}/2h_{\ell}}, & \text{cont.}, h_{\ell} \geq 0, \\ e^{-\alpha_{\ell}/2\Delta_{\mathbf{x}} h_{\ell}^{\text{d}}} c'_{\ell} \frac{e^{\alpha_{\ell} \Delta_{\mathbf{x}}}}{e^{\alpha_{\ell} \Delta_{\mathbf{x}} - 1}}, & \text{disc.}, h_{\ell} \geq 0, \alpha_{\ell} \Delta_{\mathbf{x}} > 0. \end{cases} \quad (107)$$

Lemma 21 (Measurement Noise): Given a multivariate independent exponential measurement noise $v(\mathbf{v}_k)$, the solution of (38b) is

$$E'_{k+1} = \rho_{\mathbf{v}_k}^{\text{E}}(-\mathbf{C}\mathbf{h}_{k+1,a} - \mathbf{C}\mathbf{h}_{k+1,b}) \quad (108)$$

which is independent of \mathbf{x}_{k+1} .

Proof: The proof is similar to that of Lemma 20 except $\mathbf{h}_{k+1,a} = \mathbf{h}_{k+1,b} := \mathbf{0}$ and the substitution of $\Phi \mathbf{h}_{k,a}$ by $\mathbf{C}\mathbf{h}_{k+1,a}$, $\Phi \mathbf{h}_{k,b}$ by $\mathbf{C}\mathbf{h}_{k+1,b}$ and \mathbf{w}_k by \mathbf{v}_{k+1} . ■

REFERENCES

- [1] I. Dokmanic and M. Vetterli, "Room helps: Acoustic localization with finite elements," in *Proc. IEEE Int. Conf. Acoust., Speech, Signal Process. (ICASSP)*, Kyoto, Japan, Mar. 2012, pp. 2617–2620.
- [2] T. van Waterschoot and G. Leus, "Distributed estimation of static fields in wireless sensor networks using the finite element method," in *Proc. IEEE Int. Conf. Acoust., Speech, Signal Process. (ICASSP)*, Kyoto, Japan, Mar. 2012, pp. 2853–2856.
- [3] N. Nam and R. Gribonval, "Physics-driven structured cosparseness modeling for source localization," in *Proc. IEEE Int. Conf. Acoust., Speech, Signal Process. (ICASSP)*, Kyoto, Japan, Mar. 2012, pp. 5397–5400.
- [4] F. Sawo, "Nonlinear state and parameter estimation of spatially distributed systems," Ph.D. dissertation, Universität Karlsruhe, Karlsruhe, Germany, 2009.
- [5] F. Xaver, G. Matz, P. Gerstoft, and C. F. Mecklenbräuer, "Localization of acoustic sources using a decentralized particle filter," *EURASIP J. Wireless Commun. Netw.*, vol. 2011, no. 1, 2011.
- [6] U. A. Khan and J. M. F. Moura, "Distributing the Kalman filter for large-scale systems," *IEEE Trans. Signal Process.*, vol. 56, no. 10, pp. 4919–4935, 2008.
- [7] F. Xaver, G. Matz, P. Gerstoft, and C. F. Mecklenbräuer, "Predictive state vector encoding for decentralized field estimation in sensor networks," in *Proc. IEEE Int. Conf. Acoust., Speech, Signal Process. (ICASSP)*, Kyoto, Japan, Mar. 2012, pp. 2661–2664.
- [8] S. Vasudevan, R. H. Anderson, S. Kraut, P. Gerstoft, L. T. Rogers, and J. L. Krolik, "Recursive Bayesian electromagnetic refractivity estimation from radar sea clutter," *Radio Sci.*, vol. 42, pp. 1–19, 2007.
- [9] S. M. Kay, *Fundamentals Of Statistical Signal Processing, Estimation Theory*. Hoboken, NJ, USA: Pearson Education, 1993, vol. 1.
- [10] B. Ristic, S. Arulampalam, and N. Gordon, *Beyond the Kalman Filter: Particle Filters for Tracking Applications*. Boston, MA, USA: Artech House, 2004.
- [11] O. Hlinka, O. Slučák, F. Hlawatsch, P. M. Djurić, and M. Rupp, "Likelihood consensus and its application to distributed particle filtering," *IEEE Trans. Signal Process.*, vol. 60, no. 8, pp. 4334–4349, Aug. 2012.
- [12] O. Hlinka, F. Hlawatsch, and P. M. Djurić, "Distributed particle filtering in agent networks: A survey, classification, and comparison," *IEEE Signal Process. Mag.*, vol. 30, no. 1, pp. 61–81, 2013.
- [13] A. J. Weiss and E. Weinstein, "A general class of lower bounds in parameter estimation," *IEEE Trans. Inf. Theory*, vol. 34, no. 2, pp. 338–342, 1988.
- [14] H. L. Van Trees and K. L. Bell, *Bayesian Bounds For Parameter Estimation And Nonlinear Filtering/Tracking*. New York, NY, USA: IEEE, 2007.
- [15] A. Renaux, P. Forster, P. Larzabal, C. D. Richmond, and A. Nehorai, "A fresh look at the Bayesian bounds of the Weiss–Weinstein family," *IEEE Trans. Signal Process.*, vol. 56, no. 11, pp. 5334–5352, Nov. 2008.
- [16] D. A. Koshaev and O. A. Stepanov, "Application of the Rao–Cramer inequality in problems of nonlinear estimation," *J. Comp. Syst. Sci. Int.*, vol. 36, pp. 220–227, Apr. 1997.
- [17] G. Reise and G. M. Gröchenig, "Distributed field reconstruction in wireless sensor networks based on hybrid shift-invariant spaces," *IEEE Trans. Signal Process.*, vol. 60, no. 10, pp. 5426–5439, Oct. 2012.
- [18] P. Tichavsky, C. H. Muravchik, and A. Nehorai, "Posterior Cramer–Rao bounds for discrete-time nonlinear filtering," *IEEE Trans. Signal Process.*, vol. 46, no. 5, pp. 1386–1396, 1998.
- [19] Z. Duan, V. P. Jilkov, and X. R. Li, "State estimation with quantized measurements: Approximate MMSE approach," in *Proc. IEEE 11th Int. Conf. Inf. Fusion*, 2008, pp. 1–6.
- [20] N. D. Tran, A. Renaux, R. B. S. Marcos, and P. Larzabal, "Weiss–Weinstein bound for MIMO radar with colocated linear arrays for SNR threshold prediction," *Signal Process.*, vol. 92, no. 5, pp. 1353–1358, 2012.
- [21] A. Renaux, "Weiss–Weinstein bound for data-aided carrier estimation," *IEEE Signal Process. Lett.*, vol. 14, no. 4, pp. 283–286, 2007.
- [22] I. Rapoport and Y. Oshman, "Recursive Weiss–Weinstein lower bounds for discrete-time nonlinear filtering," in *Proc. 43rd IEEE Conf. Decision Control*, Dec. 2004, vol. 3, pp. 2662–2667.
- [23] S. Reece and D. Nicholson, "Tighter alternatives to the Cramer–Rao lower bound for discrete-time filtering," in *Proc. 8th Int. Conf. Inf. Fusion*, Jul. 2005, vol. 1, p. 6.
- [24] I. Rapoport and Y. Oshman, "Weiss–Weinstein lower bounds for Markovian systems. Part 1: theory," *IEEE Trans. Signal Process.*, vol. 55, no. 5, pp. 2016–2030, May 2007.
- [25] I. Rapoport and Y. Oshman, "A new estimation error lower bound for interruption indicators in systems with uncertain measurements," *IEEE Trans. Inf. Theory*, vol. 50, no. 12, pp. 3375–3384, Dec. 2004.
- [26] I. Rapoport and Y. Oshman, "Weiss–Weinstein lower bounds for Markovian systems. Part 2: applications to fault-tolerant filtering," *IEEE Trans. Signal Process.*, vol. 55, no. 5, pp. 2031–2042, May 2007.
- [27] B. Patrick, *Probability and Measure*, 3 ed. New York, NY, USA: Wiley, 2012.
- [28] Frank and E. Burk, *A Garden of Integrals, Number 31 in The Dolciani Math. Expos.*, 1 ed. New York, NY, USA: Math. Assoc. Amer., 2007.
- [29] B. Bobrovsky and M. Zakai, "A lower bound on the estimation error for Markov processes," *IEEE Trans. Autom. Control*, vol. 20, no. 6, pp. 785–788, Dec. 1975.
- [30] K. L. Bell and H. L. V. Trees, "Combined Cramér–Rao/Weiss–Weinstein bound for tracking target bearing," in *Proc. 4th IEEE Workshop Sens. Array Multichannel Process.*, Jul. 2006, pp. 273–277.
- [31] A. Bhattacharyya, "On a measure of divergence between two statistical populations defined by their probability distributions," *Bull. Calcutta Math. Soc.*, vol. 35, no. 99–109, p. 4, 1943.
- [32] T. Kailath, "The divergence and Bhattacharyya distance measures in signal selection," *IEEE Trans. Commun. Technol.*, vol. 15, no. 1, pp. 52–60, Feb. 1967.
- [33] H. Chernoff, "A measure of asymptotic efficiency for tests of a hypothesis based on the sum of observations," *Ann. Math. Stat.*, vol. 23, no. 4, pp. 493–507, 1952.
- [34] L. M. Leemis and J. T. McQueston, "Univariate distribution relationships," *Amer. Statist.*, vol. 62, no. 1, pp. 45–53, 2008.
- [35] F. Xaver, G. Matz, P. Gerstoft, and N. Görtz, "Localization of acoustic sources utilizing a decentralized particle filter," presented at the 46th Asilomar Conf. Signals, Syst., Comput., Pacific Grove, CA, USA, Nov. 2012.
- [36] Z. Chen, "Bayesian filtering: From Kalman filters to particle filters, and beyond," *Statist.*, vol. 182, no. 1, pp. 1–69, 2003.



Florian Xaver received the B.Sc. degree in electrical engineering, the Dipl.-Ing. degree in telecommunications (2009), and the Dr. techn. degree in technical sciences (2013), with distinction, from Vienna University of Technology, Austria. In the winter term of 2007, he studied at Universidad Politécnica de Madrid, Spain.

For his diploma thesis, he had a work contract with NXP Austria Styria. From 2009 to 2013, he was with Institute of Telecommunications, Vienna University of Technology. In 2010, he spent six weeks at Scripps Institution of Oceanography, University of California, San Diego. His research interests include communications, stochastic signal processing, estimation theory, partial differential equations, wave propagation, and radio frequency identification.



Peter Gerstoft received the Ph.D. degree from the Technical University of Denmark, Lyngby, Denmark, in 1986.

From 1987 to 1992, he was with Ødegaard and Danneskiold-Samsøe, Copenhagen, Denmark. From 1992 to 1997, he was at Nato Undersea Research Centre, La Spezia, Italy. Since 1997, he has been with the Marine Physical Laboratory, University of California, San Diego. His research interests include modeling and inversion of acoustic, elastic and electromagnetic signals.

Dr. Gerstoft is a Fellow of Acoustical Society of America and an elected member of the International Union of Radio Science, Commission F.



Gerald Matz (S'95–M'01–SM'07) received the Dipl.-Ing. degree (1994) and the Dr. techn. degree (2000) in electrical engineering and the Habilitation degree (2004) for “Communication Systems” from the Vienna University of Technology, Austria.

He is currently an Associate Professor with the Institute of Telecommunications, Vienna University of Technology. He has held visiting positions with the Laboratoire des Signaux et Systèmes, Ecole Supérieure d'Electricité, France; with the Communication Theory Lab at ETH Zurich, Switzerland;

and with Ecole Nationale Supérieure d'Electrotechnique, d'Electronique, d'Informatique et d'Hydraulique de Toulouse, France. He has published some 170 scientific articles in international journals, conference proceedings, and edited books. He is co-editor of the book *Wireless Communications over Rapidly Time-Varying Channels* (New York: Academic, 2011). His research interests include wireless communications, sensor networks, statistical signal processing, and information theory.

Prof. Matz currently serves on the IEEE SPS Technical Committee on Signal Processing for Communications and Networking and on the IEEE SPS Technical Committee on Signal Processing Theory and Methods. He is Associate Editor of the IEEE TRANSACTIONS ON INFORMATION THEORY and was on the Editorial Board of the IEEE TRANSACTIONS ON SIGNAL PROCESSING, the EURASIP Journal SIGNAL PROCESSING, and the IEEE SIGNAL PROCESSING LETTERS. He was Lead Guest Editor of the Special Issue on Managing Complexity in Multiuser MIMO Systems in the IEEE JOURNAL OF SELECTED TOPICS SIGNAL PROCESSING, Technical Program Co-Chair of EUSIPCO 2004, Technical Vice-Chair of Asilomar 2013, and member of the Technical Program Committee of numerous international conferences. In 2006, he received the Kardinal Innitzer Most Promising Young Investigator Award.



Christoph F. Mecklenbräuker (S'88–M'97–SM'08) received the Dipl.-Ing. degree in electrical engineering from Technische Universität Wien, Austria, in 1992 and the Dr.-Ing. degree from Ruhr-Universität Bochum, Germany, in 1998, both with distinction. His doctoral dissertation on matched field processing received the Gert-Massenberg Prize in 1998.

He was with Siemens, Vienna, from 1997 to 2000. He was a delegate to the Third Generation Partnership Project (3GPP) and engaged in the standardiza-

tion of the radio access network for the Universal Mobile Telecommunications System (UMTS). From 2000 to 2006, he has held a senior research position with the Forschungszentrum Telekommunikation Wien (FTW), Wien, Austria, in the field of mobile communications. In 2006, he joined the Faculty of Electrical Engineering and Information Technology as a Full Professor with the Technische Universität Wien. Since 2009, he leads the Christian Doppler Laboratory for Wireless Technologies for Sustainable Mobility. He has authored approximately 100 papers in international journals and conferences, for which he has also served as a reviewer, and holds eight patents in the field of mobile cellular networks. His current research interests include vehicular connectivity, ultrawideband radio, and MIMO-techniques for wireless systems.

Dr. Mecklenbräuker is a member of the IEEE Signal Processing, Antennas and Propagation, and Vehicular Technology Societies, as well as VDE and EURASIP.